DISCUSSION PAPER SERIES

DP20141
(v. 2)

MINING DISRUPTIONS, BLOCKCHAIN SECURITY, AND THE VALUE OF BITCOIN

Sören Karau and Emanuel Moench

ASSET PRICING



ISSN 0265-8003

MINING DISRUPTIONS, BLOCKCHAIN SECURITY, AND THE VALUE OF BITCOIN

Sören Karau and Emanuel Moench

Discussion Paper DP20141
First Published 17 April 2025
This Revision 27 November 2026

Centre for Economic Policy Research
187 boulevard Saint-Germain, 75007 Paris, France
2 Coldbath Square, London EC1R 5HL
Tel: +44 (0)20 7183 8801
www.cepr.org

This Discussion Paper is issued under the auspices of the Centre's research programmes:

- Asset Pricing

Any opinions expressed here are those of the author(s) and not those of the Centre for Economic Policy Research. Research disseminated by CEPR may include views on policy, but the Centre itself takes no institutional policy positions.

The Centre for Economic Policy Research was established in 1983 as an educational charity, to promote independent analysis and public discussion of open economies and the relations among them. It is pluralist and non-partisan, bringing economic research to bear on the analysis of medium- and long-run policy questions.

These Discussion Papers often represent preliminary or incomplete work, circulated to encourage discussion and comment. Citation and use of such a paper should take account of its provisional character.

Copyright: Sören Karau and Emanuel Moench

MINING DISRUPTIONS, BLOCKCHAIN SECURITY, AND THE VALUE OF BITCOIN

Abstract

We study how exogenous disruptions to Bitcoin mining affect its market valuation. Using narrative instruments in a structural VAR, we find that negative mining shocks persistently reduce hashrate and Bitcoin valuations, accounting for up to 15 percent of the forecast error variance of Bitcoin prices. While difficulty adjustment quickly restores normal block production, valuation effects are delayed and long-lasting. We interpret these findings through a dynamic model of mining, network security, and Bayesian learning. Mining disruptions reveal information about the resilience of mining activity, affecting investors' expectations about the network's continued ability to sustain security under less favorable future mining conditions. Our results suggest that expectations about the long-run provision of security are an important determinant of Bitcoin valuations.

JEL Classification: E42, G32, L14, O16

Keywords: Bitcoin, Blockchain, Mining, Proxy var

Sören Karau - soeren.karau@bundesbank.de
Deutsche Bundesbank

Emanuel Moench - e.moench@fs.de
Frankfurt School of Finance & Management and CEPR

Acknowledgements
The views expressed in this paper are those of the authors and do not necessarily coincide with the views of the Deutsche Bundesbank or the Eurosystem. This paper supersedes a previously circulated paper entitled ``Is it Really Mine? Mining Shocks and their Effects on Bitcoin Valuations'' which can be found under https://papers.ssrn.com/sol3/papers.cfm?abstract_id=4362032. We thank seminar participants at the CEPR Fintech and Digital Currencies RPN Annual Meeting, the Cryptocurrency Research Conference, Frankfurt School of Finance & Management, the Federal Reserve Board, Deutsche Bundesbank and the International Association of Applied Econometrics.

Mining Disruptions, Blockchain Security, and the Value of Bitcoin*

Sören Karau[1] **Emanuel Moench**[2]

November 18, 2026

Abstract

We study how exogenous disruptions to Bitcoin mining affect its market valuation. Using narrative instruments in a structural VAR, we find that negative mining shocks persistently reduce hashrate and Bitcoin valuations, accounting for up to 15 percent of the forecast error variance of Bitcoin prices. While difficulty adjustment quickly restores normal block production, valuation effects are delayed and long-lasting. We interpret these findings through a dynamic model of mining, network security, and Bayesian learning. Mining disruptions reveal information about the resilience of mining activity, affecting investors' expectations about the network's continued ability to sustain security under less favorable future mining conditions. Our results suggest that expectations about the long-run provision of security are an important determinant of Bitcoin valuations.

Keywords: Bitcoin, Blockchain, Mining, Proof of Work, Blockchain Security, Proxy VAR

JEL Codes: E42, G32, L14, O16

---

*The views expressed in this paper are those of the authors and do not necessarily coincide with the views of the Deutsche Bundesbank or the Eurosystem. We thank seminar participants at the Cryptocurrency Research Conference, Frankfurt School of Finance & Management, the Federal Reserve Board, Deutsche Bundesbank and the International Association of Applied Econometrics.

[1]Deutsche Bundesbank, Wilhelm-Epstein-Straße 14, 60431 Frankfurt am Main. Contact e-mail: soeren.karau@bundesbank.de.

[2]Corresponding author. Frankfurt School of Finance & Management and CEPR, Adickesallee 32–34, 60322 Frankfurt am Main, Germany. Contact e-mail: e.moench@fs.de.

1 Introduction

Bitcoin's supply of coins follows a predetermined protocol, but the resources that secure its transaction record do not. Instead, the computational power devoted to maintaining the blockchain is supplied by miners, whose ability and willingness to operate depend on economic incentives and external conditions. This distinction raises a fundamental question for Bitcoin's valuation: does the market attach value to the continued provision of network security, and how does it respond when that provision is unexpectedly disrupted? In this paper, we use exogenous shocks to Bitcoin mining to identify their effects on Bitcoin prices and other measures of network activity. We argue that the resulting price responses are consistent with a forward-looking security channel in which investors assess the network's ability to sustain mining activity and security over time.

Proof-of-Work (PoW), introduced by Nakamoto (2008), makes the creation of new blocks computationally costly. Because altering previously recorded transactions requires competing with the computing power of honest miners, the resources devoted to mining are central to the network's resistance to attacks. This protection must be maintained continuously, not merely when a transaction is initially recorded. As Budish (2022) emphasizes, the network's security at any moment depends on the computing power devoted to maintaining it at that moment.[1] Bitcoin's design therefore differs from systems in which the infrastructure securing an asset is largely independent of the asset's own market valuation. Mining is compensated by newly issued bitcoins and transaction fees, whose value in turn depends on Bitcoin's price.

Figure 1 illustrates the resulting two-way relationship. Higher Bitcoin prices increase the value of block rewards and encourage miners to deploy additional computing power, so that *hashrate follows price* (see, e.g., Prat and Walter, 2021). But mining can potentially affect valuations in the opposite direction: the resources committed by miners contribute to the security and expected usefulness of the network, which may influence demand for Bitcoin. However, an observed correlation between hashrate and prices cannot establish this reverse effect, because mining decisions themselves respond to Bitcoin prices and to expectations about future returns. The empirical challenge is therefore to isolate changes in mining activity that are not caused by developments in Bitcoin demand or valuation. More generally, it is not obvious whether a temporary decline in hashrate should matter much for prices when the network remains highly secure. This is precisely the relationship we investigate.

We identify *mining shocks* using a narrative approach in the spirit of Romer and Romer (1989). We collect episodes in which external events plausibly disrupted aggregate mining

[1] Hashrate is not a sufficient measure of the economic cost of an attack: the resources available to potential attackers, their costs, and their incentives also matter. Nevertheless, in a given security environment, the computational resources supplied by honest miners are an important determinant of network security.

Figure 1: Feedback effects between mining and Bitcoin price

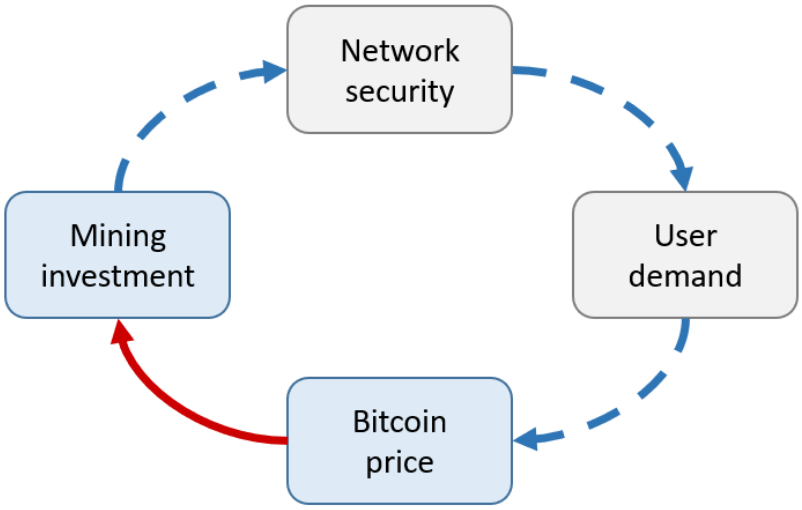

Note. Figure adapted from Chiu and Koeppl (2022) and Pagnotta (2022).

activity, including natural disasters, electricity outages, and mining-specific regulatory interventions. Their timing and associated deviations in block production provide an instrument for exogenous innovations to mining in a structural vector autoregression (VAR), identified using the external-instrument approach of Mertens and Ravn (2013) and Stock and Watson (2018). The analysis draws on weekly observations of hashrate, mining difficulty, transaction confirmation times, fees, on-chain activity, and Bitcoin prices. Our identification strategy is designed to separate the consequences of a disruption to mining from the familiar endogenous adjustment of mining activity to changes in Bitcoin's value.

The empirical responses reveal a striking contrast. A negative mining shock causes a persistent decline in hashrate and mining difficulty. Initially, block production slows and transaction confirmation times increase. Bitcoin's difficulty-adjustment mechanism, however, restores the pace of block production relatively quickly, even though the amount of computing power devoted to mining remains depressed. By contrast, transaction activity, fee revenues, and Bitcoin prices exhibit persistent negative responses. In particular, the price decline is relatively small on impact but becomes more pronounced over subsequent weeks and persists for many months. Mining shocks account for approximately 15 percent of the forecast error variance of Bitcoin prices at horizons up to one year. Hence, shocks to the provision of computational security are an economically meaningful source of variation in Bitcoin valuations, despite the protocol's ability to normalize block production.

Could this persistent price response simply reflect financially distressed miners selling their Bitcoin holdings? We examine this alternative using data on balances held by entities identified as miners. Mining shocks explain very little variation in those balances, which show no systematic decline following a negative mining shock. The evidence

therefore provides little support for miner liquidations as the explanation of our findings. We also examine the identifying assumptions extensively. The results remain similar when the instrument is constructed exclusively from physical and weather-related disruptions, which are less likely than regulatory announcements to affect Bitcoin demand directly. They are also robust to identification through changes in shock volatility, to recursive timing restrictions, to alternative event weights and other variations. Finally, jointly identifying a separate Bitcoin demand shock leaves the estimated mining responses largely unchanged, suggesting that our baseline mining shock is not capturing the demand component isolated by that exercise.

What explains the persistent effect on valuations when transaction processing has already normalized? We interpret the evidence through a dynamic extension of Pagnotta (2022)'s model of Bitcoin valuation and network security. In the static framework, mining activity and Bitcoin prices reinforce each other: a high Bitcoin price makes mining profitable, greater mining activity makes an attack more difficult, and stronger security supports the value users attach to holding Bitcoin. This complementarity can sustain multiple equilibria, including a high-price, high-security outcome. Importantly, that outcome need not remain viable if mining rewards become sufficiently unfavorable relative to costs. The model thereby connects the value of Bitcoin to the economic conditions under which mining resources can continue to secure the network.

Our dynamic model extension introduces persistent mining disruptions and uncertainty about the resilience of the mining industry. Investors observe the initial reduction in mining activity, but cannot immediately determine whether it reflects a temporary interruption or more fragile underlying mining conditions. They learn about this distinction as mining operations recover, or fail to recover, over time. The implications are forward-looking: mining conditions that suffice to sustain a secure network under current rewards may not suffice if effective mining rewards deteriorate in the future. Evidence of slow recovery can therefore lower investors' assessment of the probability that the high-security equilibrium remains viable under less favorable conditions, even while contemporaneous network security remains very high. Because Bitcoin's price reflects the expected value of future transactions, these revisions to beliefs about the network's longer-run resilience are reflected in today's valuation.

A calibrated version of the model illustrates how this mechanism can generate the distinctive timing of the empirical responses. An initial mining disruption reduces hashrate sharply while producing only a modest price decline, because the information available to investors on impact is limited. Persistently weak recovery subsequently shifts beliefs toward fragile mining conditions, increases perceived future viability risk, and leads to a larger, delayed price response. Difficulty adjustment meanwhile restores normal block production without undoing the persistent reduction in mining capacity. The model therefore illustrates how *expectations about the future provision of network security* can

transmit mining disturbances to Bitcoin valuations without requiring a substantial contemporaneous increase in the probability of a successful attack.

Our findings thus speak to a feature of PoW-based assets that is often obscured by Bitcoin's predetermined coin supply. While the issuance schedule is fixed by design, the security services associated with holding and transferring Bitcoin depend on the continued allocation of real resources by private miners. Exogenous disturbances to that allocation offer a way to establish that mining activity matters for market valuation. The model provides a mechanism through which investors price information about the persistence of security provision and its sustainability under future mining incentives. The empirical evidence identifies a causal mining-to-price relationship, which the model allows to interpret in terms of learning about future equilibrium viability.

Related Literature. Our analysis contributes first to the literature on PoW mining incentives and blockchain security. Budish (2024) studies the economic costs of majority attacks and decentralized trust, while Auer (2019) examines payment finality and the implications of declining block rewards for Bitcoin's security. Garratt and van Oordt (2023) emphasizes the role of mining-specific capital and fixed costs in discouraging attacks, and Prat and Walter (2021) studies how mining investment responds to Bitcoin prices and technological developments. While these contributions primarily examine the provision, incentives, and costs of security, we identify the effects of exogenous disruptions to mining on Bitcoin valuations and on the use of the network.

Second, we contribute to models linking cryptocurrency valuations to blockchain security. Most directly, Pagnotta (2022) derives the complementarity between mining, network security, and Bitcoin prices, with the possibility of multiple equilibria. Related contributions include Chiu and Koeppl (2022), who studies security and transaction throughput in the presence of a potential attacker, and Sockin and Xiong (2023), who examines the valuation consequences of strategic attacks and transaction frictions. Our dynamic extension to the framework in Pagnotta (2022) adds uncertainty about the persistence of mining disruptions, learning from recovery, and the risk that a high-security equilibrium cannot be sustained under less favorable future mining incentives. In this way, mining is not only an endogenous response to valuations or an amplifier of demand disturbances, but also a source of information relevant to future security and current prices. Complementary evidence on mining–price feedback following Bitcoin demand shocks is presented in Appendix B.2.

Third, we relate to empirical work on cryptocurrency prices and mining fundamentals. Liu and Tsyvinski (2020) studies cryptocurrency risk and returns, while Bhambhwani et al. (2023), Garratt and van Oordt (2023), and Ciaian et al. (2021) examine aspects of the relationship between cryptocurrency markets and mining without our structural identification strategy. Scharnowski and Shi (2021) and Stinner and Tyrell (2022) analyze

particular mining disruptions in China. Our contribution is to combine a broader event-based instrument with a structural VAR in order to trace the dynamic consequences of mining shocks, distinguish them from endogenous mining adjustments, and quantify their importance for Bitcoin price variation.

Outline. Section 2 describes the mining disruption events, VAR data, and identification strategy. Section 3 presents the dynamic effects of mining shocks, examines miner liquidations as an alternative explanation, and reports identification and specification robustness checks. Section 4 develops the security–valuation mechanism and its dynamic extension with Bayesian learning. Section 5 concludes.

2 Mining Disruptions and Empirical Strategy

We identify exogenous changes in Bitcoin mining activity using a narrative instrument constructed from disruptions to mining operations. This section describes the underlying events and their immediate effects on mining, introduces the VAR data and specification, and explains how the event information is used for structural identification.

2.1 Mining Disruption Events

We collect dated events that plausibly shift Bitcoin mining activity for reasons unrelated to contemporaneous developments in Bitcoin trading and demand. A first category (*Type-1*) consists of physical or weather-related disruptions, including floods, storms, fires, and interruptions to electricity supply. A second category (*Type-2*) comprises mining-specific interventions by authorities, such as restrictions on electricity use, closures of mining facilities, and confiscations of mining equipment. The full chronology, including the assigned direction and instrument weight of each event, is provided in Appendix Table A.1.

Three episodes illustrate the economic nature of these disturbances. Flooding in Sichuan, China, in June 2018 damaged mining facilities and reduced the computing capacity available to the Bitcoin network. After mining in the US had become more important, a Texas winter storm in February 2021 led to electricity shortages and widespread power outages that forced a suspension of mining operations in that state. These two events are examples of Type-1 physical disruptions whose occurrence was clearly independent of any changes in Bitcoin demand. The shutdown of mining facilities in Sichuan during the Chinese mining crackdown in June 2021 instead represents a Type-2 disturbance. The immediate loss of mining activity was accompanied by uncertainty about whether and how quickly operations could relocate or resume elsewhere. The latter episode is especially relevant for the persistence of mining disruptions, but also raises a

Figure 2: Mining outcomes around disruption events

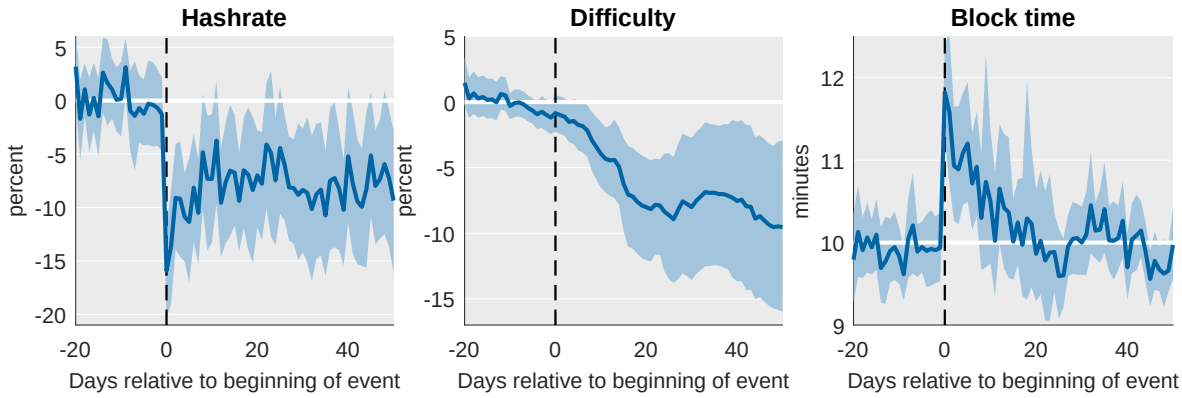

Note. The figure plots mean daily hashrate, difficulty, and average block time from 20 days before to 50 days after mining events for which the precise start date is known. Hashrate and difficulty are percentage deviations from event-specific linear trends fitted to the 60 days ending immediately before the event; block time is in minutes. Shaded areas denote pointwise 95% event-date-cluster bootstrap intervals for the mean. The vertical dashed line marks the event date; horizontal lines mark zero trend deviation or the ten-minute block-time target.

more demanding exclusion-restriction question: announcements concerning the regulatory treatment of mining could in principle influence Bitcoin demand independently of their direct effects on mining. We therefore distinguish physical disruptions from mining-specific regulatory events in our robustness analysis, and show in Section 3.3 that our main conclusions also hold when identification relies only on the former.

To examine how such events affect the network, it is useful to distinguish three closely related mining variables. The *hashrate* measures the computational effort devoted to finding valid blocks and is our measure of aggregate mining intensity. The *difficulty* determines how computationally demanding it is to find a valid block. Finally, the *block interval* is the time between successive blocks. Bitcoin's protocol targets an average block interval of approximately ten minutes, adjusting difficulty after every 2,016 blocks (roughly two weeks at the target rate). A sudden reduction in hashrate therefore initially slows block production because difficulty cannot respond immediately. At the next retargeting, difficulty falls and the average block interval moves back toward ten minutes even if the hashrate has not recovered. This protocol adjustment is important for distinguishing disruptions to transaction processing from persistent changes in the mining resources that secure the network.

Figure 2 summarizes the behavior of hashrate, difficulty, and average block time around 21 of our events for which the starting date can be determined with high precision from news reports. It plots their average paths from 20 days before to 50 days after an event, together with bootstrap confidence bands. To account for the secular increase in mining activity, hashrate and difficulty are expressed relative to event-specific trends estimated over the preceding 60 days. Hashrate falls sharply by approximately

10% around the event date and remains below its pre-event trend. Difficulty adjusts more gradually and remains depressed. By contrast, the average block interval initially rises above ten minutes but subsequently returns toward the protocol target as difficulty responds. Since retargeting occurs at different dates relative to each event, the average difficulty path adjusts smoothly even though the protocol changes difficulty discretely. These descriptive event paths thus reveal the distinction that motivates our analysis: block production can normalize while the computing resources devoted to mining remain persistently lower. We now move to using such events as narrative instruments in a structural VAR to provide a causal analysis of the dynamic effects of mining disruptions.

2.2 Data and VAR Specification

Let $\mathbf{y}_t$ denote a vector of eight weekly Bitcoin-related variables. We estimate the reduced-form VAR

$$\mathbf{y}_t = \mathbf{c} + \sum_{\ell=1}^{p} \mathbf{B}_\ell \mathbf{y}_{t-\ell} + \mathbf{u}_t, \qquad \mathbb{E}[\mathbf{u}_t] = \mathbf{0}, \quad \mathbb{E}[\mathbf{u}_t \mathbf{u}_t'] = \mathbf{\Sigma}, \tag{1}$$

where $\mathbf{c}$ is a vector of intercepts, $\mathbf{B}_\ell$ denotes the coefficient matrix for lag ℓ, and $\mathbf{u}_t$ is the vector of reduced-form innovations.

Table 1 summarizes the variables and their data sources. Four variables describe mining activity and its immediate economic environment: estimated *hashrate*, mining *difficulty*, median *transaction confirmation time*, and the total U.S. dollar value of *transaction fees*. The transaction confirmation-time measure is conceptually distinct from the average interval between mined blocks discussed above. In addition to the pace of block production, the time before a transaction is confirmed can depend on congestion in the pool of pending transactions. Similarly, fees are a component of miners' revenue, but also reflect transaction demand when users bid for scarce block space.[2] The remaining variables measure on-chain use and valuation: median transaction size in U.S. dollars, the number of transactions, the number of active addresses, and the U.S. dollar price of Bitcoin. Active addresses are a measure of network use, not a direct count of distinct users.

We average daily observations in levels for each weak. Weekly variables enter in logarithms, except for median transaction confirmation time, which is measured in minutes. We estimate the VAR in log levels, following Sims et al. (1990), to preserve possible cointegrating relationships.[3] Weekly aggregation is particularly useful because hashrate is estimated indirectly from the stochastic process of block discovery; daily estimates can be noisy even when actual mining capacity is unchanged. It also reduces possible

[2]Pending Bitcoin transactions are collected in memory pools before being included in a block. If pending demand exceeds available block space, users may face longer confirmation times even when the average interval between blocks remains unchanged.

[3]For instance, Bhambhwani et al. (2023) report evidence of cointegration between the prices and hashrates of proof-of-work cryptocurrencies.

Table 1: Main variables used in the empirical analysis

Variable	Unit/transformation	Source
Hashrate	log TH/s	blockchain.com
Difficulty	log	blockchain.com
Transaction confirmation time (median)	minutes	blockchain.com
Transaction fees (total)	log USD	blockchain.com
Transaction size (median)	log USD	bitinfocharts.com
Number of transactions	log	blockchain.com
Active addresses	log count	bitinfocharts.com
Bitcoin price	log USD	blockchain.com

Note. The table lists the variables included in the baseline VAR model, alongside their sources.

day-of-the-week effects (see Biais et al., 2023) and accommodates episodes for which the exact event day cannot be established. Appendix A.2 discusses the choice of frequency in detail, and Section 3.3 examines robustness using a daily frequency of observations. The estimation sample runs from June 3, 2013, through April 20, 2026. We use twelve weekly lags and estimate the VAR using standard Bayesian methods described in Appendix A.3.

2.3 Identification of Mining Shocks

Our object of interest is an exogenous innovation to mining activity, which we call *mining shock*. The distinction from endogenous changes in hashrate induced by Bitcoin demand is important because miners have incentives to expand or curtail their operations when the value of block rewards changes – the feedback from Bitcoin prices to mining depicted as red arrows in Figure 1.[4] We instead aim to isolate the effects represented by the blue arrow in Figure 1. To do so we use a narrative external instrument in the spirit of Romer and Romer (1989), combined with proxy VAR identification following Mertens and Ravn (2013) and Stock and Watson (2018).

We construct the instrument from the event chronology described in Section 2.1. Rather than assigning every event the same weight, we use a measure of its observed effect on block production to proxy for the size of the underlying mining disturbance, following the logic of Baker and Bloom (2013). Specifically, write $\overline{\mathrm{BT}}_t$ for the average block interval, in minutes, measured in the relevant event window, and define the signed deviation $\Delta\mathrm{BT}_t \equiv 10 - \overline{\mathrm{BT}}_t$. The weekly instrument is

$$Z_t = \Delta\mathrm{BT}_t \, \mathbb{I}_t, \tag{2}$$

where $\mathbb{I}_t$ equals one in the week of an eligible mining event and zero otherwise. In this convention, an event that reduces mining activity and lengthens block intervals receives a negative weight, whereas an event that increases mining activity and shortens block intervals receives a positive weight. For precisely dated events we calculate the deviation

[4] Complementary evidence on this feedback is presented in Appendix B.2.

Figure 3: Instrument used in the proxy VAR to identify mining shocks

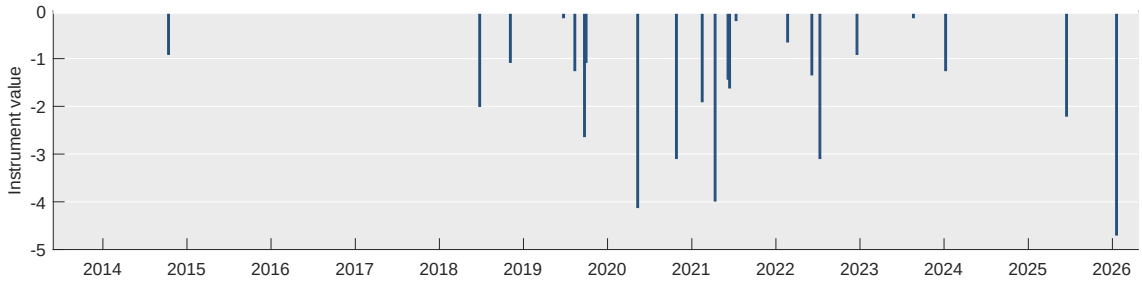

Note. Instrument values result from the weighting scheme in Equation (2), such that the dimension of the instrument corresponds to (negative) deviations in minutes from the 10-minute goal stipulated in the Bitcoin protocol.

using daily observations. When the event cannot be dated at the daily precision, we use weekly averages. We retain an event only if the observed deviation agrees in sign with the mining effect suggested by its narrative description. In the baseline analysis, this sign screen excludes four events.[5]

Figure 3 displays the resulting instrument series. Its nonzero observations identify weeks in which a documented mining event coincided with a block-time deviation of the expected sign, while the magnitudes measure the corresponding deviations in minutes. Event weights are not themselves structural shocks: the proxy VAR uses their covariance with reduced-form innovations to recover the impact direction of the latent mining disturbance.

We then use the constructed series as an external instrument – sometimes called proxy – in a VAR to isolate variations in the residuals that are due to the shock of interest, in our case exogenous changes in mining, denoted as ϵ_t^m. For an instrument series Z_t to be valid, it needs to be *relevant* and *exogenous*:

$$\mathbb{E}[Z_t \epsilon_t^{m\prime}] \neq 0, \tag{3}$$

$$\mathbb{E}[Z_t \epsilon_t^{q\prime}] = \mathbf{0}. \tag{4}$$

The condition in Equation (3) states that for an instrument Z to be relevant, it needs to be strongly correlated with the structural shock ϵ_t^m. We verify that in all specification considered, our instruments are strong, as indicated by first-stage F-statistics greater than 30 – with 44.9 in the baseline case – when regressing the instrument on the reduced-form hashrate residuals from the VAR.

The second condition in Equation (4) requires that the instrument be exogenous and thus uncorrelated with shocks ϵ_t^q that are not related to mining. This exogeneity assump-

[5]We also considered weights based on block-time changes over longer horizons and on difficulty adjustments, with similar results. Section 3.3 reports results for a binary event instrument and for weights calculated uniformly from weekly block times.

tion is particularly credible for mining disruptions caused by adverse weather or other physical events, which are plausibly unrelated to contemporaneous shocks to Bitcoin demand or other variables in the VAR. For mining-specific regulatory and enforcement actions, the assumption is less immediate. However, we stress that a concern for identification would only arise if enforcement actions – such as the confiscation of mining equipment or closure of mining facilities – were triggered by other structural shocks, for example an unexpected increase in Bitcoin demand occurring *within the same week*. We argue that this is unlikely given delays in the response and planning of enforcement actions. A related concern is that regulatory announcements could themselves convey information affecting Bitcoin demand independently of their effects on mining. We take care, however, to only include regulatory events specifically targeted to mining operations and not more broadly to Bitcoin trading or ownership. What is more, in Section 3.3, we take various steps to assuage related concerns: we show that our results are robust to using only clearly exogenous physical events, to identifying an orthogonal Bitcoin demand shock within the same VAR model, and to using an alternative identification strategy.

3 Empirical Results

We first document the dynamic effects of exogenous mining shocks in the baseline proxy VAR (Section 3.1). We then examine whether the observed price response could reflect miners liquidating their Bitcoin holdings (Section 3.2), before assessing the robustness of the mining-shock identification (Section 3.3). Additional exercises identifying a separate Bitcoin demand shock and examining mining–price feedback are presented in Appendix B.2.

3.1 Dynamic Effects of Mining Shocks

The impact of mining shocks. Figure 4 shows impulse response functions (IRFs) to a contractionary mining shock in our proxy VAR model. Mirroring Figure 2, the exogenous decrease in mining intensity leads to a highly persistent fall in the network's hashrate. Initially, the exogenous decrease in mining intensity is associated with a rise in the time it takes to solve the cryptograms and validate transactions by adding blocks to the public ledger. This leads to a drop in the difficulty level after at most two weeks, as shown in the second panel.

While both the decline in the hashrate and difficulty are highly persistent, this is not the case for transaction confirmation times in the third panel. They rise on impact by more than one minute, but the effect vanishes as the system's difficulty endogenously adjusts. After this adjustment, confirmation times even drop slightly below their initial level, likely reflecting a fall in the demand for block space. This is consistent with the

Figure 4: Impulse response functions (IRFs) to a negative mining shock

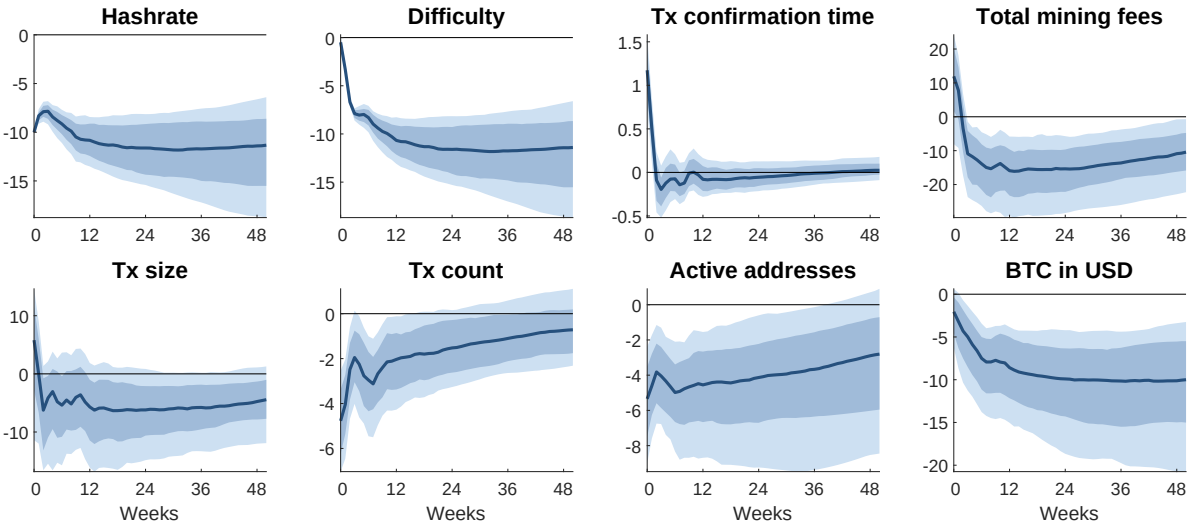

Note. Impulse responses to a mining shock identified in the proxy VAR, normalized to decrease the hashrate by 10 percent. Shaded areas denote 68% and 90% confidence bands. All values in percent, except for transaction confirmation time measured in minutes. Time sample: July 2013 to April 2026.

response of transaction fees in the fourth panel. Fee income from mining spikes on impact but decreases strongly and persistently thereafter. While the short-lived increase is again caused by slower processing of transactions until the difficulty adjustment is completed (Huberman et al., 2021; Easley et al., 2019), the protracted subsequent fall likely signals reduced transaction demand.

This interpretation is corroborated by a decline in the variables directly measuring transfer activity within the blockchain. While transaction sizes show a similar pattern as transaction fees, the number of transactions as well as the number of active addresses decline persistently. Finally, and most importantly, the price of Bitcoin drops: whereas the initial impact is small, over time Bitcoin valuations decline more strongly and remain depressed for many months after the initial shock. Hence, exogenous variations in mining activity exert a long-term impact on the price of Bitcoin.

We interpret these impulse response functions as evidence of two channels through which mining shocks impact the system. First, there is a *transaction speed channel* by which mining affects settlement speed. Higher blockchain congestion leads to higher fees, which makes it more costly to use Bitcoin to transfer value. This channel is short-lived, however, as it is shut off by the endogenous difficulty adjustment after at most two weeks. The fact that fees, blockchain activity and prices all continue to be affected long after this adjustment points instead to a second mechanism: mining fundamentals impact Bitcoin market valuations via a *security channel*. In Section 4, we show that these impulse responses are consistent with a dynamic model of Bitcoin valuation and network security. In the model, investors learn from the persistence of mining disruptions about the viability of a high-security network equilibrium, with potentially long-lived effects

Figure 5: Forecast error variance explained by mining shocks

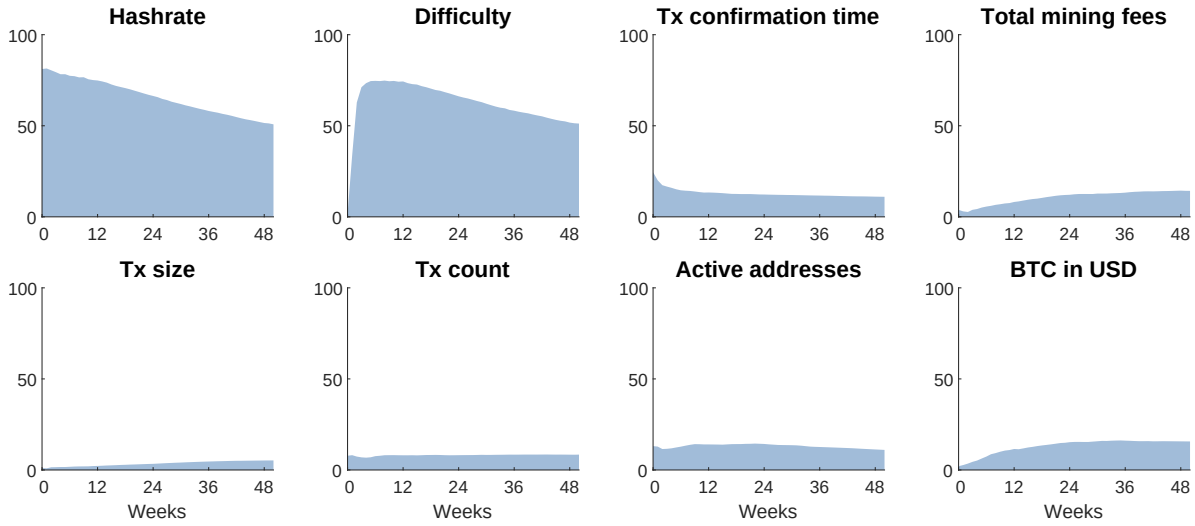

Note. FEVD to mining shock identified in the proxy VAR. Shaded areas denote 68% and 90% confidence bands. Values in percent. Time sample: July 2013 to April 2026.

on Bitcoin valuations. An alternative explanation relates to miners selling their Bitcoin holdings in response to exogenous disruptions in their activity. Before examining this explanation in Section 3.2, we quantify the extent to which variation in prices is explained by mining shocks.

Share of variation explained by mining shocks. A useful feature of our empirical framework is that it allows us to compute forecast error variance decompositions (FEVDs) to assess the quantitative importance of mining shocks for explaining variation of Bitcoin prices and the other endogenous variables in the VAR. Figure 5 provides these decompositions. The bulk of the unpredictable variation in the hashrate is explained by the mining shock in the week in which the shock occurs, with the share gradually falling to 50% over longer horizons. This shows that our identification approach captures the main drivers of mining effort. The same is true with respect to difficulty adjustments: as expected, the explained variation on impact is near zero, but rises sharply with the two-week adjustment, and then stays persistently high.

Initially, around a quarter of transaction confirmation times are captured by the mining shock, a share that drops quickly after the endogenous difficulty adjustment. The explained share of mining income from fees is about 10 to 15% in the medium run. The explained shares are somewhat lower for the size and number of blockchain transactions, but higher for active addresses, confirming that exogenous changes to mining effort have some quantitatively meaningful long-lived effects on the use of Bitcoin. Finally, and most importantly, mining shocks account for about 15 percent of the variation in Bitcoin prices at horizons up to one year. These shocks thus represent an economically significant source of Bitcoin's substantial price volatility.

Figure 6: Mining Shocks and Miner Balances

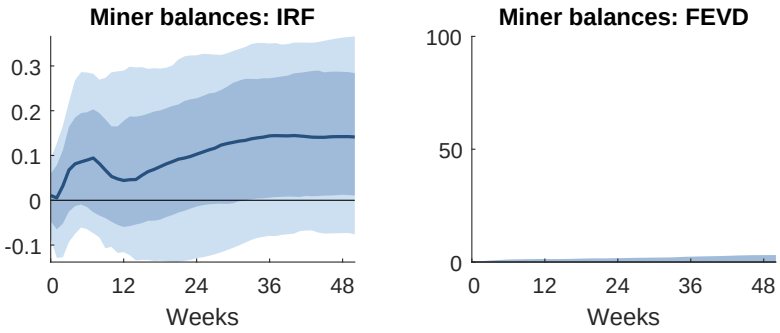

Note. Left panel: impulse response of miner balances to a negative mining shock identified in the proxy VAR, normalized to decrease hashrate by 10 percent on impact. Right panel: share of the forecast error variance of miner balances explained by mining shocks. Shaded areas denote 68% and 90% confidence bands. Values in percent. Time sample: July 2013 to April 2024.

3.2 Miner Liquidations as an Alternative Explanation

The baseline responses point to a security channel: Bitcoin prices remain depressed long after difficulty adjustment has restored normal block production. Before turning to robustness, we examine whether miner liquidations of Bitcoin could explain the persistent price effects.

Cashing out by miners. One potential alternative explanation for our findings is the liquidation of Bitcoin holdings by miners. In their detailed study of the Bitcoin blockchain, Makarov and Schoar (2021) document that miners sometimes accumulate substantial holdings of Bitcoins. When miners come under financial stress, they may sell some of these holdings, thereby exerting downward pressure on market prices. Since exogenous mining disruptions can reduce mining income or impose additional financial costs, they might also trigger such selling behavior. It is therefore important to assess whether miner liquidations could account for the persistent price effects documented in our baseline analysis.

To investigate this possibility, we rely on data from `Glassnode Studio` measuring the number of bitcoins held by entities identified as miners. We augment the baseline VAR with the logarithm of this series and estimate the response of miner balances to an identified mining shock. While identifying individual participants on the blockchain is generally difficult, miners can be tracked fairly well because newly minted bitcoins are distributed through observable coinbase transactions.[6]

Figure 6 reports the impulse response and forecast error variance decomposition

[6]Nevertheless, these estimates are unlikely to capture all miner holdings, and changes in balances need not coincide exactly with sales in the market. The series should therefore be interpreted as an imperfect but informative indicator of miners' aggregate holding behavior.

of miner balances following a negative mining shock.[7] The left panel shows that miner balances respond little to the shock. If anything, there is an increase over time, albeit not statistically distinguishable from zero. The variance decomposition in the right panel reinforces this conclusion: mining shocks account for only a negligible fraction of the variation in miner balances over the horizons considered.

These findings provide little support for miner liquidations as an important driver of the persistent Bitcoin price response to mining shocks. They do not rule out individual miners selling coins in response to adverse disruptions, but the absence of a systematic response in aggregate miner holdings makes it unlikely that this mechanism accounts for the substantial and persistent valuation effects identified in our analysis.

The absence of a systematic decline in aggregate miner holdings strengthens our interpretation of the persistent Bitcoin price response as evidence of a security-related valuation channel, rather than primarily a response to miner selling pressure. Complementary evidence on endogenous mining–price feedback, including the propagation of separately identified Bitcoin demand shocks, is provided in Appendix B.2.

3.3 Robustness and Additional Findings

In this section, we assess the robustness of our findings to alternative identifying assumptions, the selection and weighting of events, and changes in the VAR specification. We place particular emphasis on the credibility of the external instrument underlying our baseline results. As discussed in Section 2, the mining disruptions used to construct the instrument differ in the strength of their presumed exogeneity. We show that our results survive relying only on mining disruptions due to disasters and power outages, different constructions of the narrative instrument and alternative identifying assumptions.

Event selection and exogeneity. The process of constructing the instrument naturally involves some discretion in selecting relevant events. We took care to only include events that were not clearly too small to have had any plausible effect on aggregate mining or that stretch over an extended period and are therefore difficult to time. However, given the importance for identification in the proxy VAR, we now discuss additional potential concerns regarding our choice of events.

Our baseline instrument combines two types of mining disruptions. Type-1 events comprise physical and weather-related disruptions, including natural disasters and power outages, whose occurrence is plausibly unrelated to contemporaneous conditions in the Bitcoin market. Type-2 events instead consist of mining-specific regulatory and enforcement actions, such as the closure of mining facilities or the confiscation of mining equip-

[7] The responses of the other variables remain very similar to those in the baseline model, shown in Figures 4 and 5.

Figure 7: Robustness: IRFs to mining shock identified with type-1 events

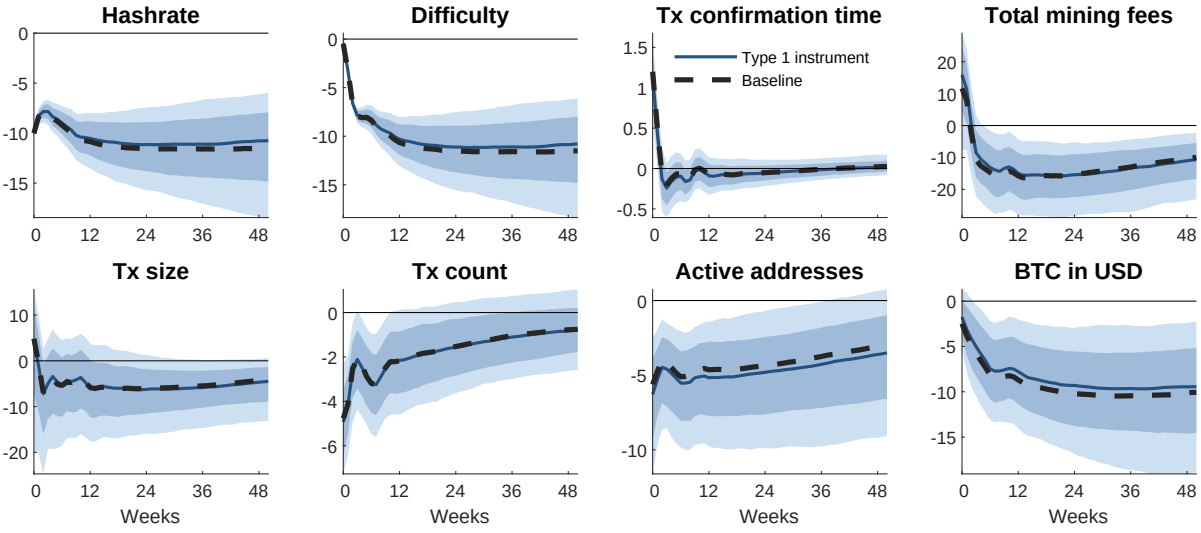

Note. Impulse responses to a mining shock identified using only type-1 events, normalized to decrease the hashrate by 10 percent. Dashed lines show responses of the baseline specification. Shaded areas denote 68% and 90% confidence bands. All values in percent, except for transaction confirmation time measured in minutes. Time sample: July 2013 to April 2026.

ment. Although the latter also provide external variation in mining activity, their validity as instruments is less immediate.

Two potential concerns arise with Type-2 events. First, regulatory interventions could themselves respond to developments in the Bitcoin market. For identification, the relevant question is whether such interventions are systematically related to contemporaneous structural shocks, rather than whether mining regulation is generally influenced by the evolution of the Bitcoin market. For example, a mining crackdown motivated by increased electricity consumption would be problematic if its timing reflected an unexpected increase in Bitcoin demand occurring within the same week. Given the planning and administrative delays typically associated with enforcement actions, we consider such contemporaneous responses unlikely. Moreover, such endogeneity would only unduly inflate our estimated price response to the extent that it was *systematic* and introduced *positive* correlation between prices and hashrate. As crackdown events are expected to reduce, not further increase, aggregate mining activity, falsely including such events in the absence of any effects on prices therefore would at best attenuate, and not amplify, our results.

Second, even predetermined regulatory interventions could convey information that affects Bitcoin valuations independently of their effects on mining. We mitigate this concern by restricting Type-2 events to interventions specifically targeting mining operations, rather than broader measures affecting Bitcoin trading or ownership. We also note that our identification does not rely on the assumption that each event captures exclusively mining-related external factors that impact the Bitcoin market. Instead, it only requires

that the instrument series does not *systematically* take up such variation. For instance, on 9 June 2021 the Chinese Qinghai province ordered local mining operations to halt – a Type-2 mining disruption – while on the same day El Salvador's Congress voted to adopt Bitcoin as legal tender – arguably a positive sentiment or demand shock, which sent Bitcoin prices sharply higher. Including this event will not undermine identification as long as the other events do not systematically correlate with similar confounding factors.

Still, to mitigate any remaining concerns we re-estimate the proxy VAR using an instrument constructed exclusively from Type-1 events. Figure 7 compares the resulting impulse responses with those from the baseline specification. The responses are remarkably similar. In particular, the negative mining shock continues to generate a persistent decline in hashrate and mining difficulty, while its effect on transaction confirmation times remains short-lived. Most importantly, Bitcoin prices decline persistently, closely tracking the baseline response. Thus, our central finding that exogenous changes in mining activity have substantial and long-lasting effects on Bitcoin valuations does not depend on the inclusion of regulatory and enforcement events.

We emphasize that the similarity of these responses also informs the interpretation of the structural mining shock. In a proxy VAR, the instrument identifies the contemporaneous impact of a latent structural shock, while its subsequent propagation is governed by the estimated dynamics of the VAR. Consequently, the fact that some Type-1 disruptions are physically short-lived does not imply that the structural response of the hashrate must be equally short-lived. The impulse response traces the effects of an initial mining innovation in the absence of subsequent structural disturbances, whereas the realized path following a particular event may also reflect additional innovations, including those associated with the recovery of mining operations.[8]

Our results thus suggest that the impact response to even shorter-lived Type-1 events can be used to identify essentially the same underlying mining shock as the broader event set. Notably, both specifications also yield a relatively small initial response of Bitcoin prices, followed by a substantially larger decline over time. This pattern is consistent with investors gradually revising their assessment of the network's longer-run viability and security as the persistence of mining weakness becomes apparent. We return to this learning mechanism in Section 4.

Finally, in Appendix B.2 we jointly identify a mining and a Bitcoin demand shock. This provides a complementary check on the exclusion restriction. If the mining instrument systematically captured general Bitcoin demand disturbances, allowing a separate instrument to identify such disturbances could materially alter the estimated mining

[8]One further way to assess whether the two classes of events capture a common mining disturbance is to recover the structural mining shock using Type-1 events alone and subsequently examine its association with Type-2 events. Indeed we find the two to be highly correlated. Since Type-2 events are not used to identify the shock in this exercise, this strong and significant association provides additional evidence that they contain the same underlying mining component.

Figure 8: Robustness: IRFs to mining shock identified using heteroskedasticity-based approach

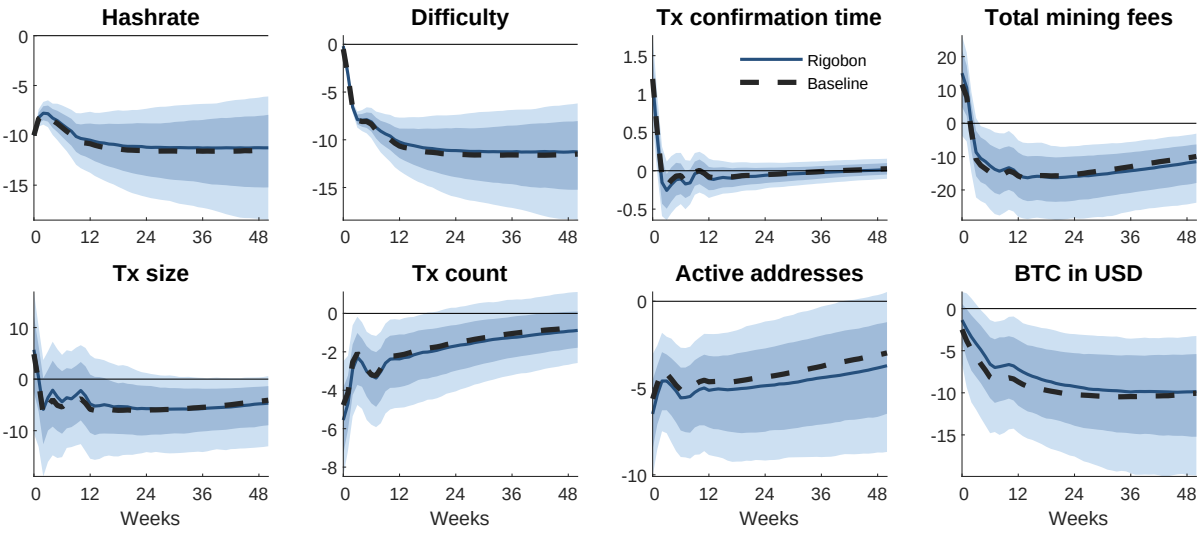

Note. Impulse responses to a mining shock identified using heteroskedasticity-based instead of external IV approach, normalized to decrease the hashrate by 10 percent. Dashed lines show responses of the baseline specification. Shaded areas denote 68% and 90% confidence bands. All values in percent, except for transaction confirmation time measured in minutes. Time sample: July 2013 to April 2026.

shock. Instead, the mining impulse responses remain very similar when both shocks are identified jointly. Since this stability is not imposed by the identification procedure, it suggests that the baseline mining shock is not materially driven by the Bitcoin demand component identified by the second instrument.

Identification through heteroskedasticity. We next consider an alternative identification approach that exploits changes in the volatility of structural shocks across different regimes, following Rigobon (2003) and Rigobon and Sack (2004). The approach has been applied to event-based identification in financial markets, including monetary and trade policy shocks (Boer et al., 2023; Wright, 2012), and more recently to stablecoin shocks by Cerutti et al. (2026). We distinguish weeks containing the narrative mining disruptions from other weeks and exploit the premise that these events increase the variance of exogenous mining innovations. Crucially, while the proxy VAR requires the narrative instrument to be orthogonal to non-mining structural shocks, identification through heteroskedasticity instead relies on the assumption that only the variance of the target shock differs systematically between event and control weeks.

In other words, the identifying assumption here is that the variance of the mining shock is higher in event weeks, while the variances of other structural shocks and the structural impact matrix remain unchanged across event and non-event weeks. With Σ^E and Σ^C denoting the covariance matrices of the VAR innovations in event and control weeks, respectively, and b_M being the impact vector of the mining shock, under these

Figure 9: Robustness: IRFs to mining shock identified recursively

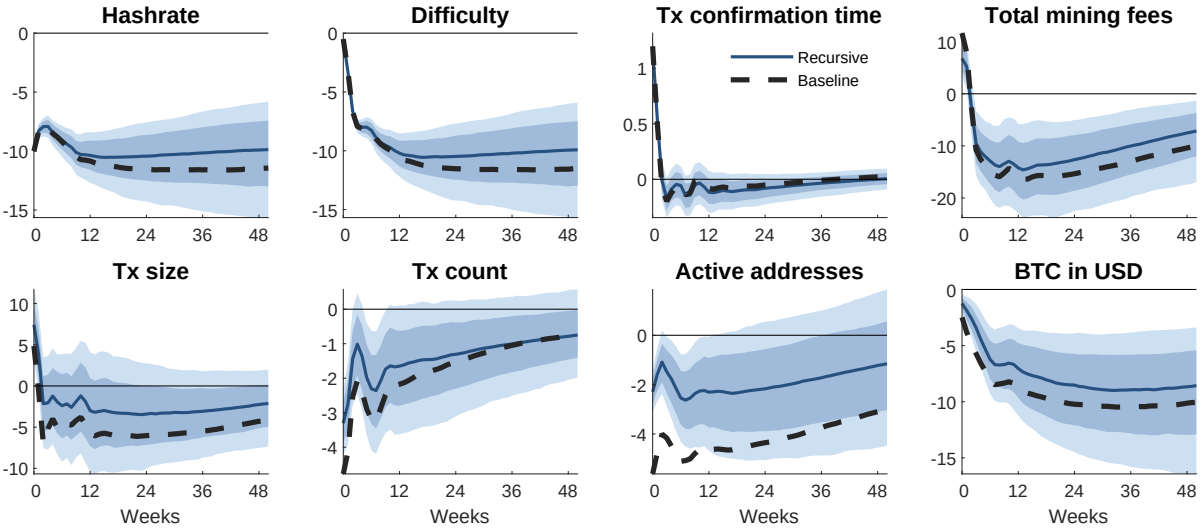

Note. Impulse responses to a mining shock identified recursively with hashrate ordered first, normalized to decrease the hashrate by 10 percent. Dashed lines show responses of the baseline specification. Shaded areas denote 68% and 90% confidence bands. All values in percent, except for transaction confirmation time measured in minutes. Time sample: July 2013 to April 2026.

assumptions their difference satisfies

$$\Sigma^E - \Sigma^C = \left(\sigma^2_{M,E} - \sigma^2_{M,C}\right) b_M b_M', \tag{5}$$

where $\sigma^2_{M,r}$ denotes the variance of the mining shock in regime r. Thus, the additional comovement of the VAR innovations in mining-event weeks identifies the mining shock's contemporaneous impact direction, up to sign and scale.[9] We use the same normalization as in our baseline analysis, imposing a 10% decline in the hashrate on impact. Appendix A.4 provides details on the identifying assumptions and their implementation.

Figure 8 shows the resulting impulse responses. They are strikingly similar to those obtained in the baseline proxy VAR. The hashrate and difficulty decline persistently, transaction confirmation times return rapidly toward their initial level, and Bitcoin prices experience a substantial and long-lasting decline. Thus, an identification strategy based on changes in structural shock variances recovers essentially the same mining-shock dynamics as the external instrument approach in our baseline analysis. This agreement provides additional support for our results under a different set of identifying assumptions.[10]

[9] We recover this direction from the event–control change in the cross-moment of VAR innovations with a control-mean-adjusted block-time measure, scaled by the change in that measure's second moment, rather than by directly estimating and diagonalizing $\Sigma^E - \Sigma^C$.

[10] To be sure, the two approaches are not fully independent, as both exploit information from the same mining disruptions. We therefore interpret the close correspondence between the estimated responses as corroborating, rather than independently establishing, the validity of our baseline identification.

Alternative identification schemes. We consider two further approaches to identifying mining shocks. First, we exploit restrictions on the speed at which miners can adjust their computational resources. As emphasized by Garratt and van Oordt (2023), mining equipment is highly specialized and involves substantial fixed costs. Installing additional hardware generally requires time, while existing equipment may continue operating even after moderate declines in mining profitability. These frictions suggest that aggregate mining activity responds only sluggishly to unexpected changes in Bitcoin prices and other demand-related variables. Indeed, the Bitcoin demand shock identified in Appendix B.2 provides direct empirical support for such a delayed adjustment.

Motivated by these considerations, we identify a mining shock recursively by ordering hashrate first in the VAR. This imposes the restriction that unexpected changes in the other variables cannot affect the hashrate contemporaneously, i.e. within the same week. As shown in Figure 9, the resulting responses are broadly similar to those from the baseline proxy VAR. In particular, the mining shock continues to have a persistent negative effect on Bitcoin valuations.[11]

Second, we estimate an internal instrument VAR in which the narrative instrument enters the VAR directly and is ordered first, following Plagborg-Møller and Wolf (2021). An important advantage of this approach is that, unlike the baseline analysis based on an external instrument and proxy VAR, it does not require the mining shock to be invertible, i.e. that it can be recovered from current and past observations of the endogenous variables in the VAR. Although commonly assumed in structural VAR analysis, this requirement may be violated if relevant information about mining shocks is not captured by the variables included in our model. As shown by Plagborg-Møller and Wolf (2021), including the instrument directly in the VAR allows for consistent estimation of normalized structural impulse responses even in the absence of invertibility.[12] Unlike the baseline external instrument approach, which uses the instrument to recover the contemporaneous impact vector of a latent mining innovation, the internal instrument specification explicitly incorporates the observed instrument process into the VAR dynamics. This may be relevant here because mining events differ in their temporal characteristics: physical disruptions are often isolated and sometimes short-lived, whereas regulatory interventions

[11] One potential concern is that sufficiently large or sustained Bitcoin price movements may induce miners to switch off or reactivate existing equipment within the same week, violating the recursive timing restriction. As an additional diagnostic, we recover the recursively identified mining shocks and estimate their price effects using local projections, excluding shocks occurring during periods of large contemporaneous price changes (above 20%), large cumulative price declines over three weeks (above 20%), sustained price movements in the same direction, or prices below recent historical peaks. The resulting price responses remain similar, suggesting that our recursive results are not driven by episodes in which immediate endogenous mining adjustments are particularly likely.

[12] The internal instrument approach requires a stronger exclusion restriction concerning the timing of shocks. However, conditional on lagged instruments and endogenous variables, the instrument must be correlated only with the contemporaneous mining shock, and not with other structural shocks or leads and lags of the mining shock (Plagborg-Møller and Wolf, 2021).

Figure 10: Robustness: IRFs to mining shock identified via internal IV

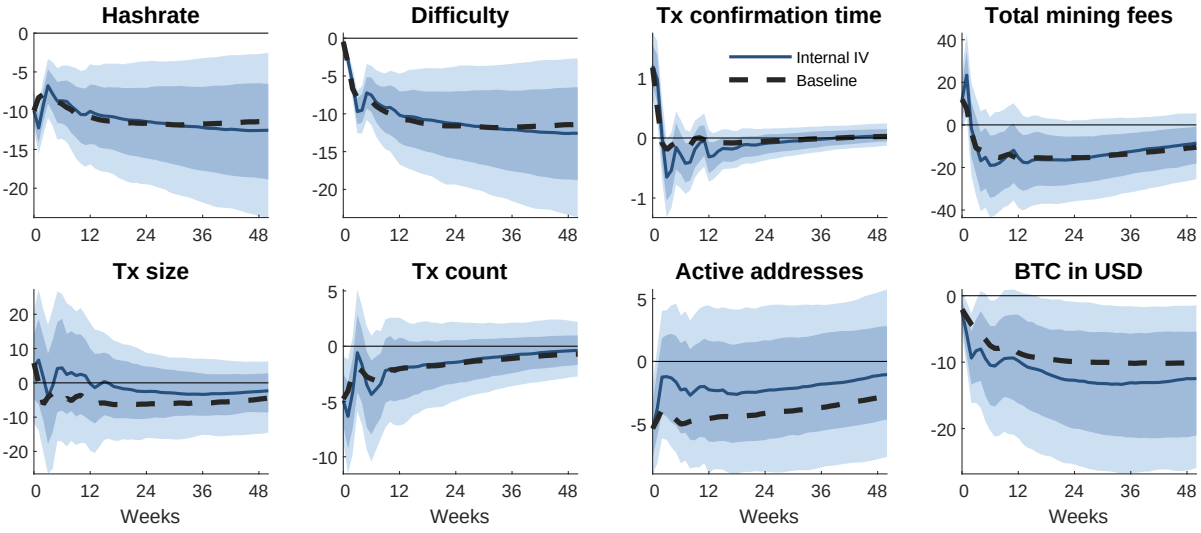

Note. Impulse responses to a mining shock identified in an internal IV VAR, normalized to decrease the hashrate by 10 percent. Dashed lines show responses of the baseline specification. Shaded areas denote 68% and 90% confidence bands. All values in percent, except for transaction confirmation time measured in minutes. Time sample: July 2013 to April 2026.

can unfold over several weeks. Such differences may matter for the estimation of the instrument's dynamics, so the two approaches need not yield identical estimates in finite samples, even if invertibility holds.

Figure 10 nevertheless shows that our findings remain intact. Mining disruptions lower hashrate and difficulty persistently, and Bitcoin prices also exhibit a pronounced and persistent negative response. The quantitative response is even somewhat larger than in the baseline, but the central conclusion that exogenous mining disturbances affect Bitcoin valuations is unaffected.

Instrument construction. We assess the sensitivity of our results to the construction of the narrative instrument, with the corresponding results reported in Appendix B.2.

Our baseline weighting scheme uses deviations in block confirmation times from the protocol's ten-minute target to capture the severity of mining disruptions. Although this provides a natural measure of their impact on mining activity, it could introduce some measurement noise because block discovery is inherently stochastic. Moreover, the baseline weighting scheme might fail to capture exogenous mining variation if in an event week other shocks drive block confirmation times in a direction inconsistent with the assigned sign of the mining shock.

First, we verify that our results are robust to using only events that lead to statistically significant deviations of block times from their ten minute target (see Appendix A.2). Second, we replace the weighted instrument with a binary indicator that records the direction of the mining disruption without distinguishing its magnitude, and without

the sign rule. Figure B.1 shows that the impulse responses do not meaningfully change. In particular, the decline in Bitcoin prices remains persistent and quantitatively similar to the baseline response. The results therefore do not appear to depend critically on using realized block confirmation times to determine the relative importance of individual events.

As a third check, we address the temporal aggregation of the instrument. In the baseline specification, we use daily block confirmation times to construct event weights where event dates can be established with sufficient precision, and weekly observations otherwise. An alternative is to consistently calculate the weights from weekly average block confirmation times, matching the frequency of the VAR. Figure B.2 shows that this change leads to somewhat smaller price effects but again leaves our overall findings largely unaffected. Hence, the main results are not driven by the precise temporal aggregation used to measure the severity of individual mining disruptions.

Data frequency. As described in Section 2 and detailed in Appendix A.2, we use weekly data for the VAR exercise to mitigate concerns over randomness in higher-frequency block time and hashrate data. However, as shown in Figure B.3, we even find evidence of persistent price effects when re-estimating the VAR using much noisier daily data.[13] Following the mining shock, the hashrate partially recovers from its initial decline but remains persistently below baseline, accompanied by a gradual adjustment in mining difficulty. While the increase in transaction confirmation times dissipates relatively quickly, Bitcoin prices decline persistently as in the baseline.

Model specifications and further robustness tests. We also verify that our findings are robust to variations in the lag length of the VAR and to the use of flat or less informative priors. Moreover, the persistent negative response of Bitcoin prices survives specifications in which hashrate and Bitcoin prices, or all potentially nonstationary variables, enter in first differences rather than log levels.[14] The same is true when we restrict the sample to before the Chinese mining ban in the Summer of 2021. Finally, as the hashrate is not directly observed but estimated from block confirmation times and difficulty levels, it is important to investigate whether our results are driven by the selected data provider of the hashrate series. This is not the case, as we obtain almost identical results when using other hashrate estimates.[15]

[13] To mitigate measurement noise arising from stochastic block discovery, we use the filtered hashrate series of Wüstenfeld and Geldner (2025). This reduces a noisy impact hashrate effect but turns out to be immaterial for the other responses.

[14] The uncertainty bands for most of the other variables become much wider, ruling out any analysis of the propagation channels.

[15] Our baseline results use series from `blockchain.com` but results are almost unchanged when instead using the series from `bitinfocharts.com` and we observe even more hashrate persistence and somewhat larger price responses when using the filtered series computed in Wüstenfeld and Geldner (2025), available at `https://janwuestenfeld.github.io/hashrate-filter/`.

Mining–price feedback and demand shocks. Finally, Appendix B.2 presents complementary evidence from a VAR in which we jointly identify mining and Bitcoin demand shocks using two external instruments. Importantly, the impulse responses to mining shocks remain almost unchanged relative to our baseline specification, even though the joint identification allows their structural impact vector to adjust (Figure B.4). This stability provides further support for our identification strategy, suggesting that the baseline mining shock is not materially contaminated by the demand component identified separately. The appendix also investigates the feedback between mining activity and Bitcoin valuations. We find that demand shocks induce delayed adjustments in mining activity, which in turn amplify their effects on Bitcoin prices (Figure B.5). Moreover, these valuation effects are more persistent when the network has previously experienced adverse mining shocks (Figure B.6). Both findings are consistent with the mining–security–valuation feedback emphasized in our theoretical framework that we turn to now.

4 Mining Shocks, Learning, and the Viability of Blockchain Security

Our empirical results reveal a striking difference between the short- and long-run effects of mining disruptions. A negative mining shock temporarily slows block production, but confirmation times recover as the protocol adjusts mining difficulty. Hashrate and Bitcoin prices, in contrast, remain depressed, with valuations responding only modestly at first and declining more substantially in subsequent weeks. In this Section, we sketch a model in which this pattern reflects the information that mining disruptions convey about the network's ability to maintain security in the future. Our starting point is the model by Pagnotta (2022), which studies the interaction between mining incentives, network security, and Bitcoin valuations. We first describe the static mechanism and its multiple equilibria from his model and then introduce persistent mining disruptions and Bayesian learning in a dynamic extension. The full model, its calibration, and the numerical solution are described in Appendix C.

4.1 Static Model of Bitcoin Value and Network Security

The model in Pagnotta (2022) features three types of agents: Bitcoin users, miners, and a potential attacker. Users value Bitcoin because it allows them to take advantage of exchange opportunities that would otherwise be unavailable. The utility from these transactions depends on the network remaining operational and its transaction record being secure. Miners compete to add blocks to the blockchain, receiving block rewards denominated in Bitcoins in exchange for using their computational resources. Finally, a potential saboteur may attempt to undermine the network by creating a competing

blockchain. If successful, such an attack destroys the usefulness, and hence the value, of Bitcoin in the model.

This environment creates a direct connection between Bitcoin valuations and mining incentives. A higher expected Bitcoin price raises the value of block rewards, encouraging miners to commit more computational resources. In the symmetric mining equilibrium, and assuming constant marginal mining costs, aggregate hashrate H_t satisfies

$$H_t = \frac{m-1}{m}\frac{\delta\psi}{\kappa}\, E_t^1[p_{t+1}], \tag{6}$$

where m is the number of miners, ψ is the block reward in bitcoins, κ denotes marginal mining costs, and δ is the discount factor. The operator E_t^1 denotes expectations conditional on the network surviving the potential attack. Equation (6) formalizes the familiar "hashrate follows price" relationship: more valuable block rewards sustain greater mining activity. The condition resembles a free-entry relationship in that more valuable block rewards induce greater aggregate mining effort.

Mining, however, also affects Bitcoin's value. The attacker is endowed with computational capacity A and aims to overcome the mining resources devoted to maintaining the legitimate blockchain. Following Pagnotta (2022), the probability of the network surviving an attack is represented by

$$S(H_t, A) = \begin{cases} 1 - \left(\dfrac{A}{H_t}\right)^k, & H_t > A, \\ 0, & H_t \leq A, \end{cases} \tag{7}$$

where k governs the number of blocks the attacker must overturn. The economic implication is that security increases with the computing power supplied by honest miners, relative to the resources available to an attacker. A larger hashrate therefore raises the likelihood that users can continue to rely on the blockchain.

To see how this feeds back into prices, suppose that Bitcoin users obtain utility $V(b)$ from real Bitcoin balances b, with V increasing and concave, and find a transaction opportunity with probability f. Let B denote the supply of bitcoins and n the mass of identical users, so that each holds B/n bitcoins in equilibrium. Their optimal demand, together with market clearing, implies

$$S(H(p_t), A)\left[fV'\left(\frac{B}{n}p_t\right) + (1-f)\delta R_{t+1}\right] = 1, \tag{8}$$

where $R_{t+1} = E_t^1[p_{t+1}]/p_t$ is the expected gross resale return conditional on the survival of the network. Investors' marginal benefit from holding Bitcoin thus consists of its expected transaction-service value and discounted resale value, both adjusted for network security. Since the level of security itself responds to Bitcoin prices through miners' investment

Figure 11: Equilibrium multiplicity of Bitcoin price and security

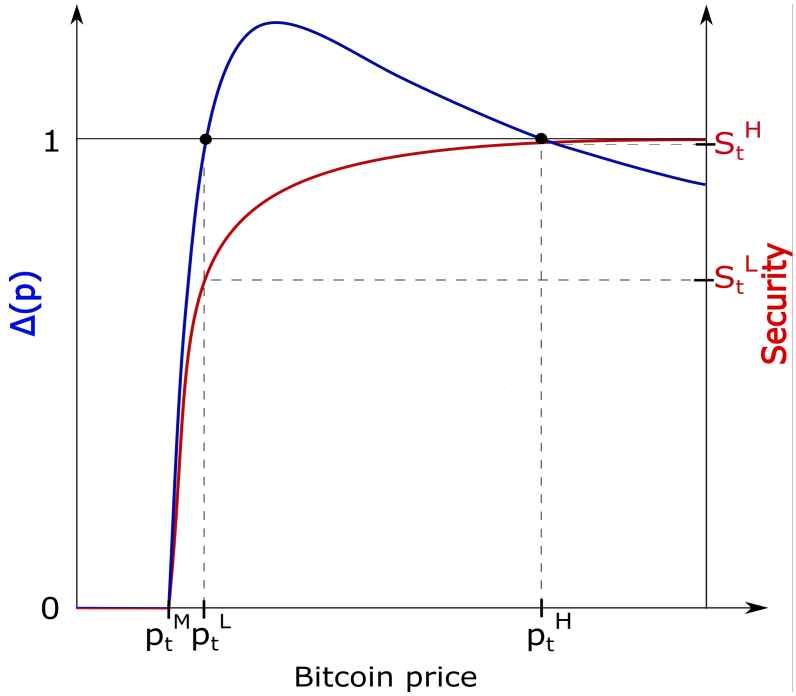

Note. Figure adapted from Pagnotta (2022). The blue curve represents the left-hand side of equation (8), denoted $\Delta(p)$; the red curve represents network security from equation (7). Equilibrium prices are given by intersections of $\Delta(p)$ with the horizontal line at one.

decisions, Equations (6)–(8) jointly determine valuations and mining activity.

The resulting complementarity can generate multiple equilibria, as illustrated in Figure 11. At a high Bitcoin price, miners earn valuable rewards and supply substantial computing power. The resulting high level of security, in turn, supports demand for Bitcoin and validates the high price. At a lower price, mining incentives weaken, security declines, and the resulting reduction in user demand can validate the low valuation. The same underlying transactional benefits and mining technology can therefore be consistent with both a low-price, low-security and a high-price, high-security equilibrium. In the figure, the two equilibria correspond to the intersections of the blue investor-demand curve with the horizontal line at one; the red curve shows how security rises with price-induced mining activity.

For our purposes, the particularly important implication is not merely that two equilibria may coexist. *The high-security equilibrium itself requires sufficiently favorable mining economics.* If the reward from honest mining becomes too small relative to its cost, the network may be unable to sustain the computing power needed to maintain this equilibrium. Consequently, information about the future profitability and resilience of mining can affect Bitcoin's value today, even if current security remains very high. This is the starting point for our dynamic extension.

4.2 Mining Disruptions, Learning, and Future Viability

We extend the static mechanism of Pagnotta (2022) in three directions. First, mining capacity does not adjust instantaneously: equipment can become temporarily unavailable, investment is gradual, and mining difficulty responds with a delay. Second, investors are uncertain about how persistent a disruption will be and learn about underlying mining conditions from the subsequent recovery of the network. Third, the mining rewards available to sustain network security may become less favorable in the future. Together, these features allow a disruption to have modest immediate valuation effects but larger consequences as investors learn about the long-run resilience of mining. Here, we only describe the ingredients and implications of the dynamic model. The full model details are provided in Appendix C.

Mining resilience and recovery. We distinguish between *installed mining capital*, such as hardware and associated infrastructure, and the portion of that capital currently available for use. A power outage, for example, can reduce effective hashrate immediately without destroying the underlying equipment. Restoring mining activity may nevertheless take time, particularly if facilities have been damaged, electricity supply remains unreliable, or equipment has to be relocated. Miners also adjust the share of available capacity they operate in response to profitability, which depends partly on mining difficulty relative to the value of Bitcoin rewards. Moreover, because expanding installed capacity takes time and depends on expected profitability, lower Bitcoin prices can discourage investment and prolong the recovery of the hashrate.

The central uncertainty that investors face concerns the *resilience of the mining industry*. We assume that its underlying conditions can be either resilient ($\theta_t = G$) or fragile ($\theta_t = B$). Under resilient conditions, mining operations recover relatively quickly from disruptions, and operating conditions remain favorable. Under fragile conditions, restoring capacity is slower, utilization is lower, and mining is less profitable. These conditions are persistent but not permanent. Importantly, investors do not observe the underlying state directly. They know that a disruption has occurred, but do not initially know whether it represents a temporary interruption or signals more enduring weakness in mining operations.

As hashrate evolves after the event, investors receive imperfect information about the recovery of the network and update their beliefs about the state. In the model, they summarize these beliefs by $\pi_t = \Pr(\theta_t = G \mid \mathcal{I}_t)$, the posterior probability that mining fundamentals are resilient. A rapid recovery makes resilient conditions more likely. Weak recovery, in turn, shifts probability toward fragility. This is a Bayesian learning mechanism: new evidence changes investors' assessment of the persistence of mining weakness, rather than the initial disruption immediately revealing its full consequences.

The model also captures the distinction between effective mining resources and the speed of transaction processing. A decline in hashrate initially increases the expected time needed to find a block because difficulty is predetermined. Bitcoin's protocol subsequently lowers difficulty, restoring the block interval toward its target. Thus, *block production can return to normal even when the network operates with persistently less computational capacity*. The information conveyed by the recovery of hashrate can remain relevant for valuations long after the immediate disturbance to block production has disappeared.

Why future reward conditions matter. Why should investors' revised beliefs about mining resilience affect Bitcoin prices substantially if the network remains secure today? The answer lies in the possibility that mining rewards will become less attractive relative to operating costs in the future. To capture this possibility, we distinguish between the current mining-reward regime and a potentially less favorable future regime, in which the effective reward available to sustain security is lower. This could reflect a reduction in the long-run security budget as block subsidies become less important, or more generally a deterioration in mining economics. We model the arrival of this stressed regime as uncertain rather than equating it with a particular scheduled Bitcoin halving. Once entered, the less favorable regime persists.

The distinction between *mining resilience* and the *reward regime* is crucial. Resilience describes how readily the industry can restore and sustain mining capacity; the reward regime describes how demanding the economic environment is in which that capacity must be maintained. Under current rewards, both resilient and fragile mining conditions may support the high-security equilibrium. Under less favorable rewards, however, only the resilient industry may be capable of sustaining sufficient mining activity. In terms of the static model, unfavorable reward-to-cost conditions can eliminate the high-mining equilibrium or leave existing capital below the level needed to remain on that equilibrium branch. Thus, learning that mining conditions are fragile raises the perceived risk of losing the high-security outcome *when future mining incentives weaken*, even if the network is presently secure.

We represent such a loss of viability by a transition to a separate, persistent low-value state. The model uses the boundary implied by the static mining–security complementarity to determine whether the high-security branch can continue under stressed rewards. The value assigned after failure of that branch is specified separately. This stylized construction isolates the economic mechanism without requiring a fully structural dynamic investment and equilibrium-selection model.

Forward-looking valuation. Bitcoin's price reflects not just its current usefulness for transactions, but also the expected value of retaining a coin for future transactions. To make this link explicit, we use logarithmic transaction utility, a special case of the

investor problem in Pagnotta (2022), and write the dynamic pricing relation as

$$p_t = S(H_t)\left\{M + \chi\, E_t\left[J_{t+1}p_{t+1} + (1 - J_{t+1})p_L\right]\right\}, \tag{9}$$

where M summarizes the current transaction-service payoff, χ discounts the continuation value, and $S(H_t)$ captures current network security. The indicator J_{t+1} equals one if the high-security branch remains viable next period; otherwise Bitcoin enters the low-value state with residual price p_L. Expectations integrate over future mining conditions, the recovery information investors may receive, and the possibility of a deterioration in mining rewards. Equation (9) is the intuitive counterpart of the recursive equilibrium pricing equation in Appendix C.

This equation reveals the main valuation channel. A moderate mining disruption changes current security only slightly if the network starts from a highly secure position. Yet evidence of persistently weak recovery can lower investors' probability that the network will withstand less favorable mining conditions in the future. Their assessment of Bitcoin's continuation value then falls, and this is reflected in the price today. *The gradual arrival of information about mining resilience can therefore generate a delayed decline in Bitcoin prices following an immediate fall in the hashrate*, even as difficulty adjustment restores normal block production. Price declines can in turn reduce utilization and discourage investment, reinforcing mining weakness. The strength of this feedback depends on how close the network is to the boundary at which the high-security equilibrium becomes unsustainable.

Illustrating the mechanism: model responses and interpretation. Figure 12 reports the responses to such a calibrated mining disruption, with details on the simulation provided in Appendix C. The first row shows hashrate, mining difficulty, transaction confirmation time, and the Bitcoin price; the second row displays installed mining capital, perceived and simulated mining fragility, and the perceived risk of losing the high-security equilibrium. All paths are conditional on no viability test actually occurring over the displayed horizon.[16]

The disruption is calibrated to reduce the hashrate by approximately 10% on impact, as in the VAR, while difficulty is initially unchanged. Expected transaction confirmation time increases by more than one minute on impact, but the effect dissipates rapidly as difficulty adjusts to the lower hashrate. Hashrate initially recovers part of its decline before weakening again, ending roughly 11% below its counterfactual path after one year. Difficulty eventually follows a similar trajectory. Installed mining capital also falls grad-

[16]Importantly, this conditioning applies only to realized histories: investors' equilibrium price policy continues to incorporate the possibility of a future test. The three probability panels report percentage-point differences from the corresponding un-shocked paths. We show responses to additional paths in Figure C.1.

Figure 12: Responses to a Negative Mining Shock in the Dynamic Model

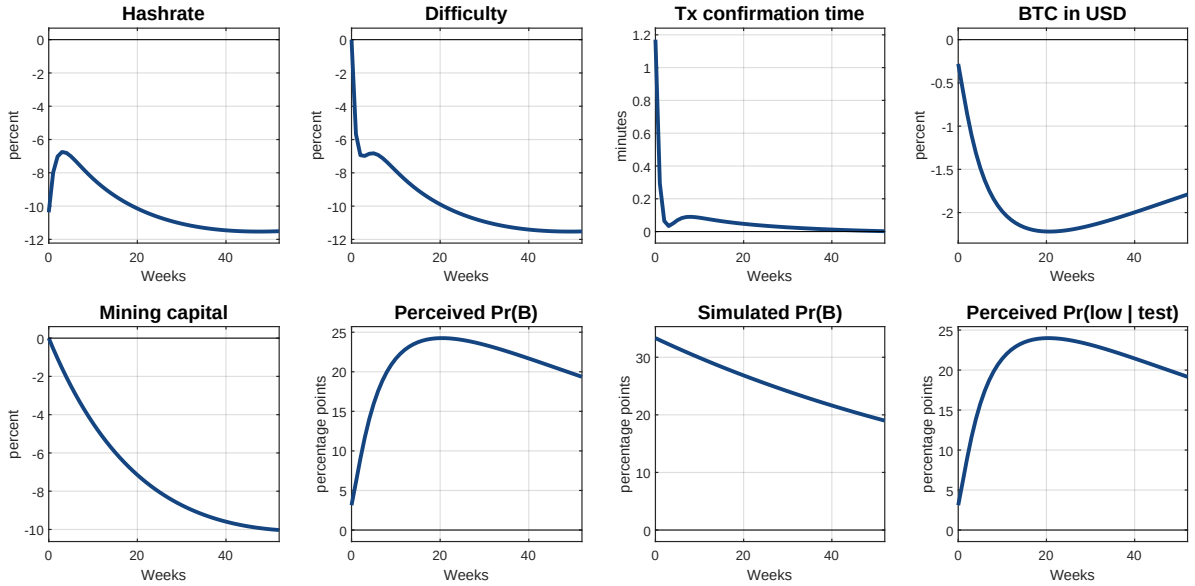

Note. The figure shows responses to a calibrated negative mining disruption in the dynamic model with Bayesian learning. All responses are measured relative to the unshocked benchmark and are conditional on no realized mining viability test during the displayed horizon. "Perceived Pr(B)" denotes investors' posterior probability of fragile mining fundamentals, whereas "Simulated Pr(B)" denotes the actual share of fragile states in the selected simulated event histories, which is not observed by investors. "Perceived Pr(low | test)" measures investors' perceived probability of losing the high-security equilibrium conditional on a viability test occurring, rather than the unconditional probability of entering the low-value state in a given week.

ually, reaching a decline of approximately 10% after 52 weeks. Thus, the normalization of block production does not imply that mining capacity has recovered: difficulty can adjust to persistently lower computing power, while slow capital adjustment and unfavorable mining conditions prolong the reduction in hashrate.

The lower panels illustrate the model's learning mechanism. The simulated share of histories with fragile mining fundamentals is substantially elevated immediately after the disruption: it is approximately 40% in the selected event class, compared with about 7% in the no-shock benchmark. Investors, however, do not observe the latent event-selection criterion. Based on the public information available on impact, their perceived probability of fragile fundamentals rises only modestly. As mining recovery proves unexpectedly weak, investors revise their beliefs: relative to the unshocked path, the perceived probability of fragility increases by approximately 24 percentage points around week 20, before declining gradually. The simulated share of fragile states also decreases over time as the latent state follows its Markov transition law, but remains elevated throughout the year.

These belief revisions translate into a higher perceived risk that the high-security equilibrium would fail *if* mining rewards were to enter the stressed regime. As shown in the bottom-right panel, the increase in this conditional failure probability closely tracks the increase in perceived mining fragility. It is not the unconditional probability of collapse in any given week, which also depends on the relatively small probability that a

viability test actually arrives. Nevertheless, the possibility of such a future event enters today's Bitcoin valuation. The price consequently declines by only about 0.3% on impact, but the response deepens to approximately -2.2% after 21 weeks, before moderating to around -1.8% after one year. This delayed repricing occurs even though no viability test is realized in the plotted histories and contemporaneous network security remains high.

The simulation thus reproduces the qualitative contrast at the center of our empirical findings: a sharp mining contraction and short-lived disruption to block production coexist with persistent weakness in mining capacity and a delayed Bitcoin price decline. The mechanism is not a large contemporaneous increase in attack risk, but the information that mining recovery conveys about the network's ability to sustain high security under less favorable future incentives. We emphasize that physical persistence partly reflects calibrated recovery and capital-adjustment rules, and that the simulated price response is smaller than its empirical counterpart. Nevertheless, the exercise illustrates how mining disruptions can have sizable valuation effects through a security channel: by revealing information about the resilience of mining activity, they alter investors' assessment of whether the network can sustain its high-security equilibrium under less favorable future mining conditions, even when contemporaneous network security remains high.

5 Conclusion

Bitcoin's supply of coins is governed by its protocol, but the computational resources that secure its transaction record depend on miners' economic incentives and operating conditions. We examine whether disturbances to this provision of security affect Bitcoin valuations. Using exogenous mining disruptions as narrative instruments in a structural VAR, we find that negative mining shocks persistently reduce hashrate and Bitcoin prices. Although block production initially slows, difficulty adjustment restores transaction processing relatively quickly. The valuation effects, by contrast, are delayed and long-lasting. Mining shocks account for up to 15 percent of the forecast error variance of Bitcoin prices at horizons of up to one year. The results are robust across several identification and specification checks.

To interpret these findings, we extend the security–valuation framework in Pagnotta (2022) to allow for persistent mining disruptions and Bayesian learning about mining resilience. A disruption may initially reveal little about how readily mining capacity can recover. As investors observe the subsequent recovery, they update their assessment of whether the network can sustain a high-security equilibrium under potentially less favorable future mining incentives. Because Bitcoin's value reflects expected future transaction services, such revisions can affect current prices even when contemporaneous network security remains very high. Our calibrated model illustrates how this mechanism can generate a small initial price response followed by a more pronounced decline.

The interpretation in terms of learning and future equilibrium viability is a model-based explanation of the empirical evidence, not a mechanism that our identification strategy measures directly.

A broader implication is that the decentralized provision of security is economically relevant to Bitcoin's market valuation. The need to attract computing resources from privately motivated miners is central to proof of work, but it also exposes the network to disruptions in the conditions under which those resources are supplied. These need not result in a successful attack or a prolonged interruption of block production to matter for valuations. In this sense, our findings suggest both that Bitcoin's security arrangements contribute to its economic characteristics and that their dependence on mining incentives constitutes a potential source of vulnerability.

Looking ahead, changes in block subsidies, transaction-fee revenue, mining technology, electricity costs, or regulatory conditions could affect the incentives to supply hashpower (Auer, 2019; Budish, 2024). Our results do not imply that such developments will necessarily undermine Bitcoin's security: adjustments in mining technology, location, and profitability may offset adverse pressures. Rather, they suggest that changes in the expected long-run economics of security provision may be relevant for market valuations. Determining how these forces will evolve is beyond the scope of our analysis.

References

Auer, R. (2019). Beyond the doomsday economics of 'proof-of-work' in cryptocurrencies. *BIS Working Papers*, 765.

Auer, R., Cornelli, G., Doerr, S., Frost, J., and Gambacorta, L. (2023). Crypto trading and Bitcoin prices: evidence from a new database of retail adoption. *BIS Working Papers*, 1049.

Baker, S. R. and Bloom, N. (2013). Does Uncertainty Reduce Growth? Using Disasters as Natural Experiments. *NBER Working Papers*, 19475.

Bhambhwani, S. M., Delikouras, S., and Korniotis, G. M. (2023). Blockchain characteristics and cryptocurrency returns. *Journal of International Financial Markets, Institutions and Money*, 86:101788.

Biais, B., Bisière, C., Bouvard, M., Casamatta, C., and Menkveld, A. J. (2023). Equilibrium Bitcoin Pricing. *Journal of Finance*, 78(2):967–1014.

Boer, L., Menkhoff, L., and Rieth, M. (2023). The multifaceted impact of US trade policy on financial markets. *Journal of Applied Econometrics*, 38(3):388–406.

Budish, E. (2022). The Economic Limits of Bitcoin and Anonymous, Decentralized Trust on the Blockchain. *Becker Friedman Institute Working Papers*, 2022-83.

Budish, E. (2024). Trust at scale: The economic limits of cryptocurrencies and blockchains. *The Quarterly Journal of Economics*, 140(1):1–62.

Cambridge Centre for Alternative Finance (2021). New data reveals timeline of china's bitcoin mining exodus. https://www.jbs.cam.ac.uk/2021/new-data-reveals-timeline-of-chinas-bitcoin-mining-exodus, accessed: 2025-03-20.

Cerutti, E. M., Firat, M., Hengge, M., and Sagawa, T. (2026). Stablecoin shocks. IMF Working Paper 2026/044, International Monetary Fund.

Chiu, J. and Koeppl, T. (2022). The Economics of Cryptocurrencies: Bitcoin and Beyond. *Canadian Journal of Economics*, 55:1–37.

Ciaian, P., d'Artis Kancs, and Rajcaniova, M. (2021). Interdependencies between Mining Costs, Mining Rewards and Blockchain Security. *mimeo*.

Easley, D., O'Hara, M., and Basu, S. (2019). From mining to markets: The evolution of bitcoin transaction fees. *Journal of Financial Economics*, 134(1):91–109.

Garratt, R. J. and van Oordt, M. R. C. (2023). Why fixed costs matter for proof-of-work–based cryptocurrencies. *Management Science*, 69(11):5284–5307.

Giannone, D., Lenza, M., and Primiceri, G. E. (2015). Prior Selection for Vector Autoregressions. *The Review of Economics and Statistics*, 97(2):436–451.

Huberman, G., Leshno, J. D., and Moallemi, C. (2021). Monopoly without a Monopolist: An Economic Analysis of the Bitcoin Payment System. *Review of Economic Studies*, 88, 3011–3040.

Karau, S. (2026). Relative monetary policy and exchange rates. mimeo.

Liu, Y. and Tsyvinski, A. (2020). Risks and Returns of Cryptocurrency. *The Review of Financial Studies*, 34(6):2689–2727.

Ma, J., Gans, J. S., and Tourky, R. (2018). Market Structure in Bitcoin Mining. *NBER Working Papers*, 24242.

Makarov, I. and Schoar, A. (2021). Blockchain Analysis of the Bitcoin Market. *NBER Working Paper*, 29396.

Mertens, K. and Ravn, M. O. (2013). The Dynamic Effects of Personal and Corporate Income Tax Changes in the United States. *American Economic Review*, 103(4):1212–1247.

Nakamoto, S. (2008). Bitcoin: A Peer-to-Peer Electronic Cash System. Technical report.

Pagnotta, E. S. (2022). Decentralizing Money: Bitcoin Prices and Blockchain Security. *The Review of Financial Studies*, 35(2):866–907.

Piffer, M. and Podstawski, M. (2018). Identifying Uncertainty Shocks Using the Price of Gold. *Economic Journal*, 128(616):3266–3284.

Plagborg-Møller, M. and Wolf, C. K. (2021). Local Projections and VARs Estimate the Same Impulse Responses. *Econometrica*, 89(2).

Prat, J. and Walter, B. (2021). An Equilibrium Model of the Market for Bitcoin Mining. *Journal of Political Economy*, 129(8):2415–2452.

Rigobon, R. (2003). Identification through heteroskedasticity. *The Review of Economics and Statistics*, 85(4):777–792.

Rigobon, R. and Sack, B. (2004). The impact of monetary policy on asset prices. *Journal of Monetary Economics*, 51(8):1553–1575.

Romer, C. D. and Romer, D. H. (1989). Does Monetary Policy Matter? A New Test in the Spirit of Friedman and Schwartz. In *NBER Macroeconomics Annual 1989, Volume 4*, NBER Chapters, pages 121–184. National Bureau of Economic Research, Inc.

Scharnowski, S. and Shi, Y. (2021). Bitcoin Blackout: Proof-of-Work and the Centralization of Mining. *mimeo, https://ssrn.com/abstract=3936787*.

Sims, C. A., Stock, J. H., and Watson, M. W. (1990). Inference in Linear Time Series Models with Some Unit Roots. *Econometrica*, 58(1):113–144.

Sockin, M. and Xiong, W. (2023). A model of cryptocurrencies. *Management Science*, 69(11):6684–6707.

Stinner, J. and Tyrell, M. (2022). Proof-Of-Work Consensus Under Exogenous Distress: Evidence from Mining Shocks in the Bitcoin Ecosystem. *Mimeo*.

Stock, J. H. and Watson, M. W. (2018). Identification and Estimation of Dynamic Causal Effects in Macroeconomics Using External Instruments. *Economic Journal*, 128(610):917–948.

Wright, J. H. (2012). What does monetary policy do to long-term interest rates at the zero lower bound? *The Economic Journal*, 122(564):F447–F466.

Wüstenfeld, J. and Geldner, T. (2025). Bitcoin hashrate dynamics: Filtering Poisson-luck and identifying responses to price and fees. SSRN Working Paper 5786322.

A VAR Data and Estimation

A.1 Mining Shock Events

Table A.1: Mining shock events used to construct instrument

Date	Event	Type	Sign	Weight
14.10.2014	Bitcoin mining facility in Thailand destroyed in a major fire	1	-1	-0.91
27.06.2018	Floods in Sichuan, China, destroy bitcoin mining centers.	1	-1	-2.00
07.11.2018	Cryptocurrency mining farms in Chinese provinces Xinjiang and Guizhou shut down for "tax inspections".	2	-1	-1.08
27.06.2019	Iranian authorities seize mining machines amid power consumption spike.	2	-1	-0.14
17.08.2019	Floods in Sichuan, China cause damage to Bitcoin mining operations.	1	-1	-1.25
23.09.2019	Hashrate plummets temporarily, while Chinese authorities conduct inspections in Inner Mongolia to close 'illegal' mining operations; national Government of Kyrgyzstan orders the cutting off of power of at least 45 large mining farms.	2	-1	-2.63
30.09.2019	Major fire at a Bitcoin mining farm in China; roughly $10M worth of mining equipment is lost. Afterwards no block found for roughly 2 hours.	1	-1	-1.08
17.05.2020	Bitcoin mining farms in Sichuan turn off machines due to weather-related hydropower shortages: the rainy season was delayed, river inflows were low, high temperatures lifted electricity demand, and power dispatch/rationing hit high-load users including mines.	1	-1	-4.12
26.10.2020	Rainy season in China ends and Chinese Sichuan pools migrate to Xinjiang, Inner Mongolia or abroad, which is hampered by COVID-19-related restrictions.	1	-1	-3.09
11.01.2021*	Iranian police confiscate some 45,000 bitcoin mining machines that were illegally using subsidized electricity.	2	-1	0.25†
16.02.2021	Most Bitcoin mining farms in Texas go offline amid largest forced power outage in U.S. history from winter storm.	1	-1	-1.90
16.04.2021	Flood in Chinese coal mine that miners rely on for energy causes subsequent safety inspections by Chinese authorities leading to enforced electricity blackout.	1	-1	-3.98
09.06.2021	China's Qinghai and Xinjiang provinces order crypto-mining operations to shut down immediately.	2	-1	-1.43
18.06.2021	Sichuan authorities order shutdown of 26 mining farms. Before hopes that China bans only dirty mining (coal powered farms in Inner Mongolia and Xinjiang) but not the hydro-powered Sichuan farms.	2	-1	-1.61
12.07.2021*	Ukraine authorities shut down largest illegal crypto mining farm in the country; Malaysian police seize more than 1000 mining rigs and destroy them with steamroller after alleged electricity theft by miners.	2	-1	-0.20
27.09.2021*	Iranian government lifts previous ban on mining for cryptocurrency for licensed operators.	2	1	-0.60†
15.11.2021*	Kyrgyzstan Shuts Down Cryptocurrency Farm With 2,500 Mining Rigs.	2	-1	-0.02
27.12.2021*	Iranian government renews ban on cryrptocurrency mining over blackouts concerns; Malaysian authorities seize more than 1,700 mining rigs in major electricty theft crackdown.	2	-1	0.05†
03.01.2022*	Kazakhstan's government temporarily cuts internet connection amid escalting protests; Kosovo bans Bitcoin mining amid energy crisis.	2	-1	-0.01
02.02.2022	Bitcoin miners power down operations in Texas amid winter storm.	1	-1	0.59†
21.02.2022*	Kazakh authorities terminate 13 cryptocurrency mining operations, announces crackdown in weeks to come, in which over 100 more crypto mining farms are shut down.	2	-1	-0.65
12.06.2022	Bitcoin mining operations in Texas go down after storm damage at Hardin Generating Station powering Marathon's site	1	-1	-1.34
13.07.2022	Texas heatwave and energy crunch curtails Bitcoin mining as miners voluntarily power down operations. Difficulty dropped ~5% as miners powered down; Texas-driven curtailments also linked to a study-estimated ~18% temporary reduction in global crypto mining activity.	1	-1	-3.09
23.12.2022	Winter Storm Elliott affects US Bitcoin mining in multiple states. Network hashrate fell >30% over the holiday weekend. In Texas alone, large flexible loads (incl. miners) curtailed from ~1,530 MW to ~130 MW (~92% cut).	1	-1	-0.91
23.08.2023	Texas heatwave affect power supply: miners voluntarily curtailed power use during periods of peak demand; Riot curtailed >95% of power usage and Marathon cited increased shutdown activity in Texas due to record-high temperatures.	1	-1	-0.14
14.01.2024	Texas winter storm hits mining activity ; Estimates from ~25% drop over ~3 days up to ~34%.	1	-1	-1.25
17.06.2025	U.S. heatwave / summer power curtailments: Bitcoin network hashrate declined in June as miners curtailed operations in response to weather-related power stress, especially in Texas.	1	-1	-2.20
24.01.2026	Bitcoin miners halt operations amid winter storm Fern; ~14% drop network-wide; major pools down ~60%.	1	-1	-4.69

Note. Type 1 denotes physical or weather disruptions; type 2 denotes mining-specific closures or enforcement. *Sign* is the recorded binary mining-shock sign. *Weight* is the pre-filter (10 - average block time), in minutes; block time is measured on the exact event date when known and over the event week otherwise. * Exact date unknown: the Monday of the event week is shown. † Sign-mismatched weight, set to zero in the VAR instrument.

Table A.2: Event surprises used to construct Bitcoin demand instrument

Date	Event	Value (%)
05.01.2017	PBOC warns against irrational Bitcoin investment after meeting major Chinese exchanges.	-11.23
11.01.2017	PBOC launches spot inspections of Chinese bitcoin exchanges.	-4.68
10.03.2017	SEC rejects the Winklevoss Bitcoin ETF.	-15.76
31.10.2017	CME announces plan to launch Bitcoin futures.	1.90
01.12.2017	CME self-certifies Bitcoin futures for Dec. 18 launch.	4.94
07.03.2018	SEC warns that many crypto trading platforms may be unlawful unless registered.	-8.48
08.03.2018	Japan FSA punishes several crypto exchanges after the Coincheck hack.	-7.07
14.03.2018	Google bans cryptocurrency-related advertising.	-3.74
10.06.2018	Coinrail hacked.	-6.96
20.06.2018	Bithumb hacked: about $32 million in digital assets stolen.	-2.11
22.08.2018	SEC rejects nine Bitcoin ETF proposals, then says it will review the staff decision.	-3.34
05.09.2018	Goldman Sachs reportedly scraps or delays plans to open a crypto trading desk.	-5.39
25.04.2019	NY Attorney General obtains court order against Bitfinex/Tether over an alleged $850 million shortfall.	-6.51
08.05.2019	Binance hacked: 7,000 BTC stolen.	-1.89
13.05.2019	Flexa launches crypto-payments network for mainstream stores.	6.47
22.11.2019	China central bank launches a fresh crypto-trading crackdown in Shanghai.	-5.52
21.10.2020	PayPal launches crypto buying/holding and merchant-use plan; would allow customers to hold BTC and other coins and use them at merchants.	2.48
29.01.2021	Elon Musk adds Bitcoin to his Twitter bio.	12.31
08.02.2021	Tesla discloses a $1.5 billion BTC purchase and intent to accept BTC payments.	11.49
11.02.2021	BNY Mellon announces a crypto custody initiative and Mastercard indicates crypto support.	2.38
13.05.2021	Tesla stops accepting BTC payments because of energy concerns.	-3.19
18.05.2021	China bans financial and payment institutions from providing crypto-related services.	-2.89
24.09.2021	China declares crypto transactions illegal and bans overseas exchanges from serving Chinese residents.	-4.62
08.11.2022	Binance signs a non-binding deal to buy FTX.com after FTX faces a liquidity crunch and roughly $6 billion in withdrawals over 72 hours.	-5.82
09.11.2022	Binance walks away from the FTX acquisition.	-5.31
14.11.2022	Binance announces creation of a crypto industry recovery fund.	5.08
05.06.2023	SEC sues Binance and Changpeng Zhao over alleged securities-law violations.	-3.66
29.08.2023	Grayscale wins court ruling against SEC over spot Bitcoin ETF rejection.	5.43
21.02.2025	Bybit hacked: roughly $1.5 billion in ETH stolen.	-1.16
02.03.2025	Trump names BTC, ETH, XRP, SOL, and ADA for a U.S. strategic crypto reserve.	7.80

Note. Dates refer to CE(S)T. *Value* is the BTC/USD price change in percent from 60 minutes before to 60 minutes after the event.

A.2 On the Choice of Weekly Data

The hashrate as a measure of total mining effort cannot be observed directly. Instead, estimates are based on block confirmation times, i.e. the time intervals that it took to add blocks to chain, relative to the 10-minute goal when taking into account the current difficulty level.[17] The process of finding solutions to cryptograms involves randomness. Hashrate estimates will therefore vary over time even when the actual total mining effort is constant. The choice of the most appropriate data frequency is therefore directly tied to how large the random fluctuations in block confirmation times are. In the following we look at empirical examples and then simulate block confirmation times and from that conclude that weekly time spells are most appropriate for our empirical analysis.

Figure A.1 shows block confirmation times on 14 January 2022, a randomly chosen day without any known mining disruptions and without a difficulty adjustment. Roughly 160 blocks were added to the blockchain on that day, slightly more than the 144 that would be expected based on the 10-minute goal per block. One striking feature is the large standard deviation, with some cryptograms being solved after one minute, while others took almost 50.

Figure A.1: Observed block confirmation times on 14 January 2022

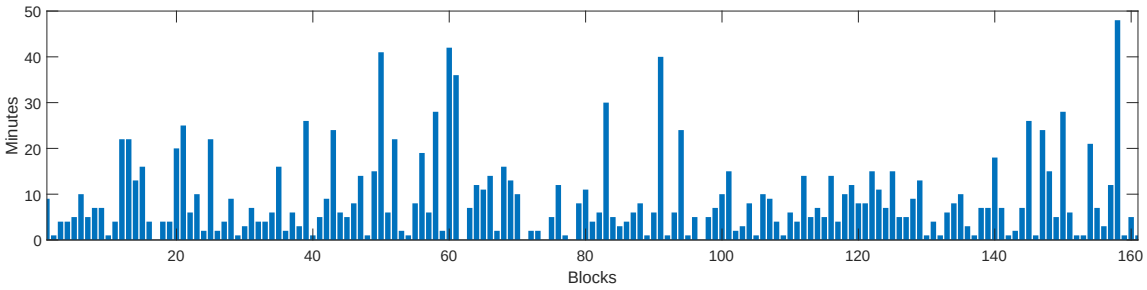

In order to assess to which degree this randomness translates into data of lower frequency, we rely on simulations. The success of solving cryptograms can be modeled by a Poisson distribution, such that the waiting time until the kth block follows a Gamma distribution (see for instance Ma et al., 2018). Specifying the parameters such that the average block confirmation time is ten minutes, we create artificial data for one hypothetical day in Figure A.2. The picture looks very similar to the empirically observed one, indicating a good model fit.

We then compute daily averages over 100 days and contrast this with weekly averages in the first panel of Figure A.3. Although, by construction, mining fundamentals are constant in these simulations, there are still large fluctuations in average daily block confirmation times, which vary between eight and twelve minutes. In other words, even fairly large empirically observed variation in daily hashrate data will often simply reflect

[17] For instance, coinmetrics.io calculates its hashrate estimate (in terra hashes per second) as $(bc/144) \times K \times (2^3 2/10^{12})/600)$, in which bc is the daily number of added blocks and K is the difficulty.

Figure A.2: Simulated block confirmation times for one day

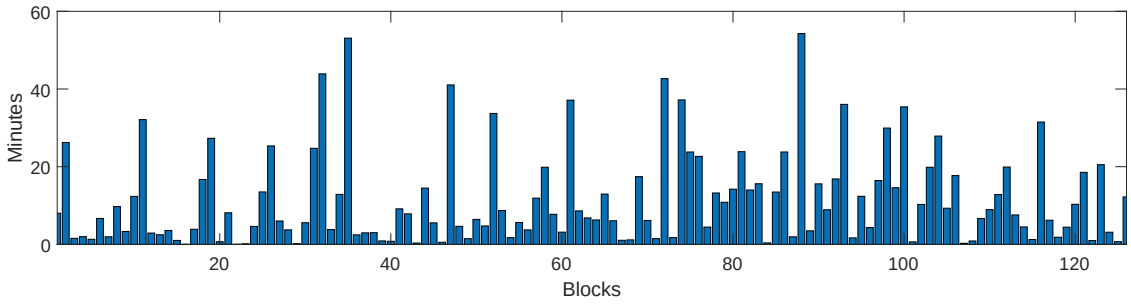

noise. In contrast, weekly averages are more stable (second panel), such that a given observed deviation from the 10-minute goal is much more likely to reflect actual changes in aggregate mining effort. Taken together with the fact that for many of our events we cannot precisely establish a single day when the respective incident happened, we therefore specify our model in weekly frequency. This reflects common practice both on analytical cryptocurrency websites as well as academic analyses.[18]

Figure A.3: Simulated block confirmation times: daily and weekly

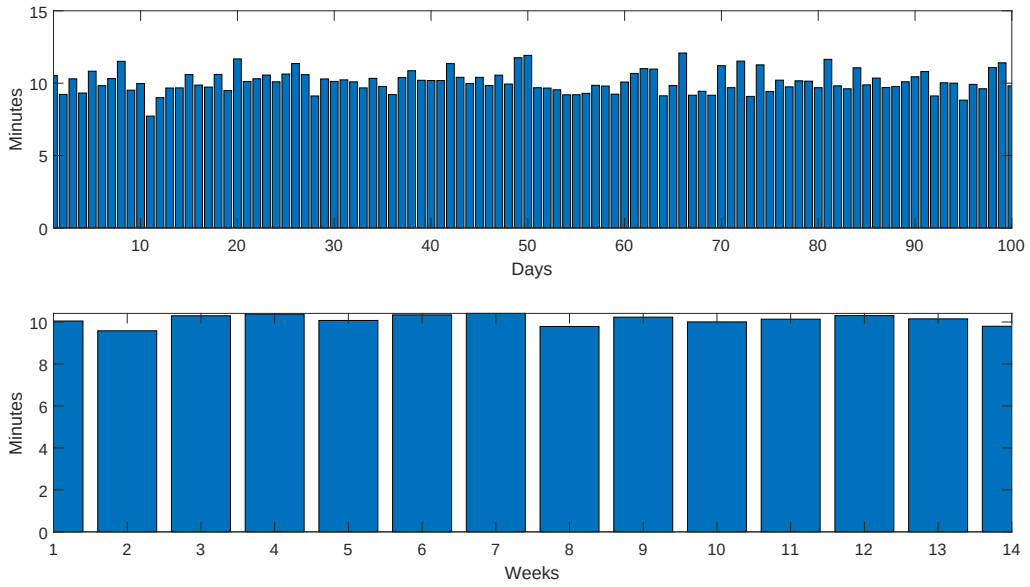

Finally, we use our simulation exercise in order to refine our instrument in an additional robustness check. Specifically, we exclude all events in which the observed variation in the average block interval did not deviate statistically significantly from ten minutes. In order to derive a confidence band, we simulate 50,000 blocks and find that weeks with deviations of more than 0.63 minutes lie outside the 90% band.

[18]Common cryptocurrency websites often suggest to use smoothed or weekly data. Biais et al. (2023) use weekly data in their empirical analysis as well, also in order to avoid day-of-the-week effects.

A.3 VAR Estimation

Proxy VAR Model Description. The main analysis is based on a structural VAR model represented by

$$\mathbf{A}_0\mathbf{y}_t = \mathbf{k} + \mathbf{A}_1\mathbf{y}_{t-1} + ... + \mathbf{A}_p\mathbf{y}_{t-p} + \epsilon_t, \quad \epsilon_t \sim \mathcal{N}(\mathbf{0}, \mathbf{I}),$$

where $\mathbf{y}_t$ is an $(n \times 1)$ vector of endogenous variables, and $\mathbf{k}$ is a vector of constants. The corresponding reduced-form VAR is:

$$\mathbf{y}_t = \mathbf{c} + \mathbf{B}_1\mathbf{y}_{t-1} + ... + \mathbf{B}_p\mathbf{y}_{t-p} + \mathbf{u}_t, \quad \mathbf{u}_t \sim \mathcal{N}(\mathbf{0}, \mathbf{\Sigma}),$$

with $\mathbf{c} = \mathbf{A}_0^{-1}\mathbf{k}$ and $\mathbf{B}_i = \mathbf{A}_0^{-1}\mathbf{A}_i$ and $\mathbf{u}_t = \mathbf{A}_0^{-1}\epsilon_t$.

Building on Stock and Watson (2018) and Mertens and Ravn (2013), we partition the shock vectors into those mining shocks, ϵ_t^m, and any other structural innovations, $\epsilon_t^{q\prime}$, with corresponding residual vectors $\mathbf{u}_t = [u_t^m, \mathbf{u}_t^{q\prime}]'$. Denoting the impact matrix $\mathbf{A}_0^{-1}$ as $\mathbf{S}$, the interest lies in that set of coefficients, column $\mathbf{s}$, that measures the initial impact to a structural mining shock. In what follows, we denote as $\mathbf{s}^q$ the initial impact of ϵ_t^p on $\mathbf{u}_t^q$, while s^m is the corresponding impact on the reduced-form mining residual u_t^m.

As outlined in the main text, to construct the instrument series we collect a list of incidents that were plausibly exogenous but are likely to have had a sizable impact on aggregate mining effort. For these instruments to be valid, the instrument series $\mathbf{Z}_t$ needs to be *relevant* and *exogenous* as follows:

$$\mathbb{E}[Z_t\epsilon_t^{m\prime}] \neq 0, \tag{A.1}$$

$$\mathbb{E}[Z_t\epsilon_t^{q\prime}] = \mathbf{0}. \tag{A.2}$$

To estimate impulse responses to a structural mining policy shock, we obtain estimates of $\mathbf{s}$ as follows. We extract the residuals $\mathbf{u}_t$ from the reduced-form VAR and use them in a two-stage least squares regression which include $\mathbf{Z}_t$ as instruments. In the first stage, u_t^m is linearly projected on $\mathbf{Z}_t$, delivering the fitted values $\hat{u}_t^m$. The latter, which are by assumption orthogonal to the remaining shocks ϵ_t^q, can be used in the second-stage regression:

$$\mathbf{u}_t^q = \frac{\mathbf{s}^q}{s^m}\hat{u}_t^m + \xi_t. \tag{A.3}$$

This procedure ensures that $\frac{\mathbf{s}^q}{s^m}$ is consistently estimated and can be used to obtain $\mathbf{s}$. We then normalize s^m so that the initial increase in the hashrate is equal to 10 percent. Given the high number of parameters to be estimated and in order to avoid overfitting, we estimate the proxy VAR via Bayesian methods using standard macro-econometric priors as described next.

Bayesian Estimation. We estimate the reduced-form VAR using a conjugate normal–inverse-Wishart prior with Minnesota-style shrinkage. Let Y be the $T \times n$ matrix of observations after the VAR lags, and let X contain an intercept and p lags of all n variables. Writing the reduced-form system as

$$Y = XC + U, \tag{A.4}$$

C is a $(1 + np) \times n$ coefficient matrix, and the rows of U have covariance matrix Σ. Let s_j^2 be the residual variance from a univariate regression of variable j on an intercept and its own first lag. We use these preliminary estimates to set the scales of the prior. The prior is

$$\Sigma \sim \mathcal{IW}(\underline{S}, \underline{\nu}), \qquad \mathrm{vec}(C) \mid \Sigma \sim \mathcal{N}(\mathrm{vec}(\underline{C}), \Sigma \otimes \underline{V}), \tag{A.5}$$

where $\underline{\nu} = n + 2$ and

$$\underline{S} = (\underline{\nu} - n - 1)\,\mathrm{diag}(s_1^2, \ldots, s_n^2) = \mathrm{diag}(s_1^2, \ldots, s_n^2). \tag{A.6}$$

Under this inverse-Wishart parameterization, the prior mean of Σ is $\mathrm{diag}(s_1^2, \ldots, s_n^2)$. The choice $\underline{\nu} = n + 2$ ensures that this mean exists; it does not imply that the variance of Σ exists.

The prior mean $\underline{C}$ is zero except for the coefficient on each variable's own first lag, which is set to one. The intercept has a zero prior mean and a large prior variance. Conditional on Σ, the prior covariance across regressors is

$$\underline{V} = \lambda^2 \begin{bmatrix} \lambda_C & 0 \\ 0 & [\mathrm{diag}(1^2, \ldots, p^2) \otimes \mathrm{diag}(s_1^2, \ldots, s_n^2)]^{-1} \end{bmatrix}, \tag{A.7}$$

where the large value of λ_C makes the prior on the intercept weakly informative. To make the implied shrinkage explicit, let $(B_\ell)_{ij}$ denote the coefficient on variable j at lag ℓ in the equation for variable i. Then

$$\mathbb{E}[(B_\ell)_{ij} \mid \Sigma] = \begin{cases} 1, & i = j,\ \ell = 1, \\ 0, & \text{otherwise}, \end{cases} \qquad \mathrm{Var}[(B_\ell)_{ij} \mid \Sigma] = \frac{\lambda^2}{\ell^2} \frac{\Sigma_{ii}}{s_j^2}. \tag{A.8}$$

Thus, more distant lags receive tighter priors, and the scale s_j^2 adjusts for the units of the predictor. Coefficients in different equations need not be conditionally independent: their prior covariance reflects the corresponding off-diagonal element of Σ.

Conditional on a chosen value of λ, conjugate updating gives

$$\bar{V} = (\underline{V}^{-1} + X'X)^{-1}, \qquad \bar{C} = \bar{V}(\underline{V}^{-1}\underline{C} + X'Y), \qquad \bar{\nu} = \underline{\nu} + T. \tag{A.9}$$

For a fixed prior, the corresponding inverse-Wishart scale can be written as

$$\bar{S} = \underline{S} + (Y - X\bar{C})'(Y - X\bar{C}) + (\bar{C} - \underline{C})'\underline{V}^{-1}(\bar{C} - \underline{C}). \tag{A.10}$$

The conditional posterior has the same normal–inverse-Wishart form:

$$\Sigma \mid Y \sim \mathcal{IW}(\bar{S}, \bar{\nu}), \qquad \mathrm{vec}(C) \mid \Sigma, Y \sim \mathcal{N}\Big(\mathrm{vec}(\bar{C}), \Sigma \otimes \bar{V}\Big). \tag{A.11}$$

In the baseline, the overall tightness λ is selected by maximizing its marginal posterior, which combines the VAR marginal likelihood with a hyperprior on λ in the spirit of Giannone et al. (2015) but we find very similar results when fixing λ at a conventional value of 0.2.

For each retained draw, we draw Σ from its inverse-Wishart posterior and the coefficient matrix from the conditional matrix-normal posterior, retaining stable VAR draws. We recompute the reduced-form innovations and identify the structural shock using the external instrument procedure described above.

We obtain the impulse response bands by pairing each retained draw of the VAR parameters with one wild resample of the observations used for proxy identification. For each matched week t, we multiply the VAR innovation vector $u_t^{(b)}$ and the instrument vector z_t by the same independent Mammen weight $\omega_t^{(b)}$, so that $(u_t^{*(b)}, z_t^{*(b)}) = \omega_t^{(b)}(u_t^{(b)}, z_t)$. We re-estimate the proxy-based impact vectors from these weighted observations and propagate them using the corresponding VAR draw. The corresponding confidence bands therefore account for both parameter estimation uncertainty and uncertainty in the proxy-based identification of the shocks. Using a residual-based moving block bootstrap delivers very similar bands.

A.4 Mining-Shock Identification through Heteroskedasticity

We provide details on the identification-through-heteroskedasticity argument used in Section 3.3. The motivating covariance argument follows Rigobon (2003), Rigobon and Sack (2004), and the SVAR application in Cerutti et al. (2026, Appendix B.2). We then describe the moments used in our implementation.

Let u_t denote the $n \times 1$ vector of reduced-form innovations from the weekly VAR. Suppose that

$$u_t = B\varepsilon_t = b_M \varepsilon_t^M + \sum_{j \neq M} b_j \varepsilon_t^j, \tag{A.12}$$

where b_M is the contemporaneous impact vector of the mining shock. Consider an event regime E and a control regime C. The benchmark identification argument assumes that the impact matrix B is constant across regimes, structural shocks have zero conditional

means and are mutually uncorrelated within each regime, and only the variance of the mining shock changes:

$$\sigma^2_{M,E} > \sigma^2_{M,C}, \qquad \sigma^2_{j,E} = \sigma^2_{j,C} \quad \text{for all } j \neq M. \tag{A.13}$$

Writing $\Sigma^r = \mathrm{Var}(u_t \mid r) = B\Omega^r B'$ for $r \in \{E, C\}$, these assumptions imply

$$\Delta\Sigma \equiv \Sigma^E - \Sigma^C = \left(\sigma^2_{M,E} - \sigma^2_{M,C}\right) b_M b_M'. \tag{A.14}$$

Thus, the covariance difference has rank one in population, and its nonzero eigenvector identifies the impact direction up to sign and scale. If e_H selects the log-hashrate innovation and $e_H' b_M \neq 0$, the direction can be normalized to a unit hashrate impact as

$$\widetilde{b}_M = \frac{\Delta\Sigma\, e_H}{e_H' \Delta\Sigma\, e_H} = \frac{b_M}{e_H' b_M}. \tag{A.15}$$

This covariance-difference representation motivates the exercise; our implementation uses the related cross-moment ratio described next, rather than estimating $\Delta\Sigma$ and extracting its leading eigenvector.

The event regime consists of weeks dated as Type 1 or Type 2 mining events in the narrative event calendar used to construct our pooled mining instrument. Control weeks are those more than one week away from every such event week. Both regimes are restricted to weeks with an observed mining-response measure and usable VAR innovations, after allowing for the VAR lags. Regime assignment uses the event dates, not the size or sign of the realized VAR innovation. In particular, an event remains in the event regime if the weighting rule used for the external instrument assigns that event a zero instrument value.

Our mining-response measure is based on observed block-production time. Let $\mathrm{BT}_t^{\mathrm{wk}}$ denote the weekly mean block time in minutes, and define

$$m_t = (10 - \mathrm{BT}_t^{\mathrm{wk}}) - \mu_C, \tag{A.16}$$

where μ_C is the mean of $10 - \mathrm{BT}_t^{\mathrm{wk}}$ over eligible control weeks, excluding the initial observations used as VAR lags. The measure is observed in both regimes; it is not the narrative instrument, which is mechanically zero outside event weeks.

For each set of estimated VAR innovations, the implemented impact-direction estimator is

$$\widehat{d}_M = \frac{\widehat{\mathbb{E}}[m_t u_t \mid E] - \widehat{\mathbb{E}}[m_t u_t \mid C]}{\widehat{\mathbb{E}}[m_t^2 \mid E] - \widehat{\mathbb{E}}[m_t^2 \mid C]}. \tag{A.17}$$

The expectations in Equation (A.17) are unweighted sample averages within each regime. They are *uncentered cross- and second moments*, rather than sample covariances and

variances. Weeks with a zero realized value of m_t remain in their assigned regime.

To see the connection with the benchmark argument, suppose that the observed response can be represented contemporaneously as $m_t = a_M \varepsilon_t^M + \sum_{j \neq M} a_j \varepsilon_t^j + \xi_t$, with $a_M \neq 0$. In addition to the restrictions in Equation (A.13), suppose that the relevant conditional means are zero and that the loadings, measurement-error moments, and cross-moments involving ξ_t are stable across regimes. If the mining-shock variance is the only source of a difference in the moments in Equation (A.17), its population counterpart equals b_M/a_M. Dividing by its log-hashrate element then recovers the unit-hashrate impact direction $b_M/(e_H' b_M)$. These conditions are substantive for our observed block-time measure: subtracting its control-regime mean does not make it a VAR innovation or ensure a zero event-regime mean. In particular, predictable movements in block time must not drive the event–control moment differences.

The estimator orients the impact vector so that its log-hashrate element is positive and normalizes that element to one. For comparison with our baseline impulse responses, we then display a mining contraction with a -0.10 log-point impact on hashrate, approximately a ten-percent decline. Subsequent responses are obtained using the estimated VAR moving-average coefficients.

The plotted central responses are pointwise medians of the retained responses obtained by pairing each Bayesian VAR draw with one resampling of the event and control observations. Within each draw, event-week pairs (m_t, u_t) are sampled with replacement individually. Control-week pairs are sampled with replacement in moving blocks of four consecutive eligible weeks. The event and control sample sizes and the narrative regime classification are held fixed. We recalculate the moments in Equation (A.17), normalize the resulting impact vector, and compute the impulse responses using that draw's VAR coefficients. Resamples with a nonpositive event-minus-control second-moment difference are excluded.

The 68% and 90% shaded regions are pointwise percentile intervals across the valid resampled responses; the central curve is their pointwise median. We incorporate uncertainty about the event–control moments used to identify the mining shock by resampling the observed block-time responses together with their corresponding VAR innovations within the two regimes for each retained VAR draw. The bands therefore reflect variation in the VAR draws and sampling variation in the identifying moments. If fewer than ten valid resampled responses remain, the code instead uses the original posterior-draw percentiles. This procedure conditions on the observed event calendar and does not re-estimate the VAR within each resample; it is therefore distinct from a full residual-based moving-block bootstrap.

The principal identifying limitation is that changes in non-mining shock variances, structural cross-covariances, the impact matrix, or the relationship between block time and contemporaneous shocks can also change the moments in Equation (A.17). The code

records the event and control second moments of m_t and their ratio, but does not estimate the covariance difference in Equation (A.14) or test its rank-one implication. Similarity between these impulse responses and the external-instrument responses should therefore be read as robustness across two identifying approaches, conditional on their respective assumptions, rather than as a direct test of the selective variance-shift restriction.

B Additional VAR Results

B.1 Further Robustness Tests

Alternative instrument construction. As discussed in Section 3.3, we first assess whether our findings depend on the weighting of mining events by observed deviations in block confirmation times. Such deviations provide information about the magnitude of mining disruptions, but are also affected by the randomness inherent in block discovery. We therefore construct a binary instrument that retains only the direction of each event, without using information about its measured severity. Figure B.1 shows that the resulting impulse responses are very similar to those of the baseline specification. In particular, the persistent negative response of Bitcoin prices remains largely unchanged, indicating that our findings do not depend on the precise event weights.

Figure B.1: Robustness: IRFs to mining shock with binary instrument

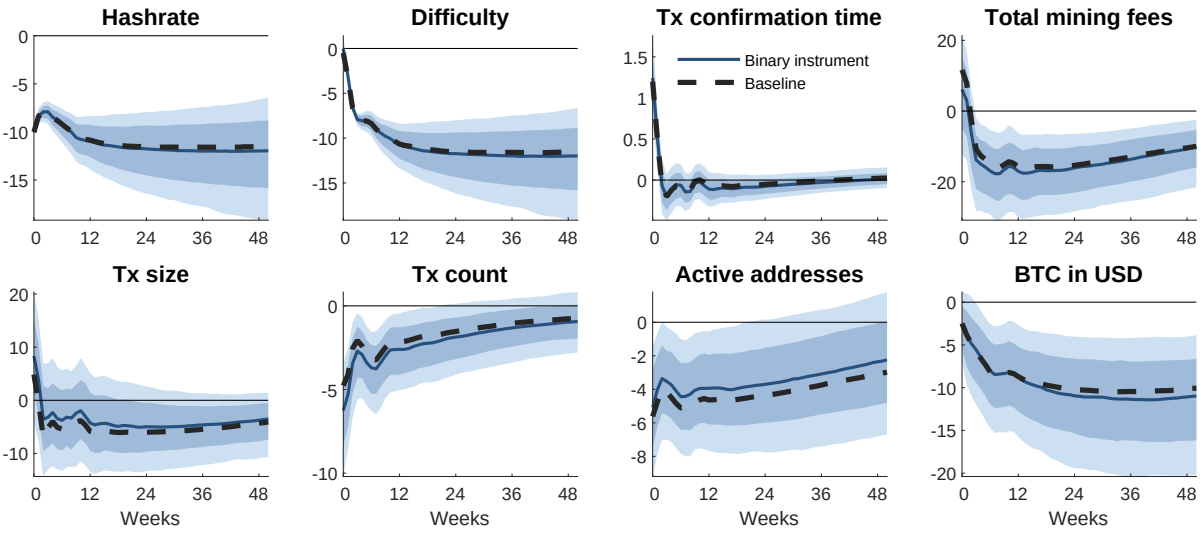

Note. Impulse responses to a mining shock identified using binary instead of weighted instrument, normalized to decrease the hashrate by 10 percent. Dashed lines show responses of the baseline specification. Shaded areas denote 68% and 90% confidence bands. All values in percent, except for transaction confirmation time measured in minutes. Time sample: July 2013 to April 2026.

We next address the temporal aggregation used to measure the severity of mining disruptions. Rather than combining daily and weekly block confirmation times depending on the precision with which events can be dated, we construct instrument weights consistently from weekly averages. As shown in Figure B.2, this alternative produces somewhat smaller Bitcoin price responses, but preserves their persistent negative pattern. Hence, the results are not particularly sensitive to the frequency at which the narrative instrument is constructed.

Daily VAR specification. Finally, we examine whether our findings depend on the use of weekly data. Weekly aggregation is particularly useful for reducing measurement

Figure B.2: Robustness: IRFs to mining shock with weekly instrument

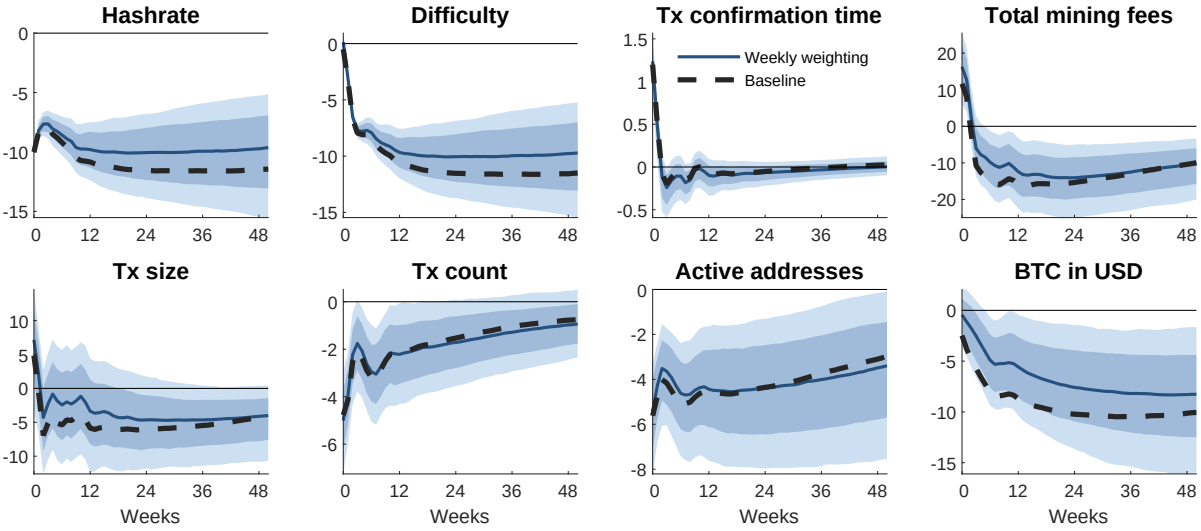

Note. Impulse responses to a mining shock identified using instrument weighted with average weekly block confirmation times for all events, normalized to decrease the hashrate by 10 percent. Dashed lines show responses of the baseline specification. Shaded areas denote 68% and 90% confidence bands. All values in percent, except for transaction confirmation time measured in minutes. Time sample: July 2013 to April 2026.

noise in hashrate, which is inferred from the stochastic process of block discovery. Nevertheless, we re-estimate the model at daily frequency, using the filtered hashrate measure of Wüstenfeld and Geldner (2025) to mitigate this noise. We specify $p = 21$ lags to make sure that the lag structure encompasses the full 2-week period of difficulty adjustments. Figure B.3 shows that the main results carry over to the daily specification. Hashrate declines persistently despite some initial recovery, while difficulty adjusts gradually and the increase in transaction confirmation times is short-lived. Most importantly, Bitcoin prices again exhibit a persistent negative response. The qualitative agreement with the weekly benchmark suggests that our findings are not an artifact of temporal aggregation.

B.2 Bitcoin Demand Shocks and Mining–Price Feedback

The main text documents persistent valuation effects of exogenous mining disruptions and finds little evidence that these effects are explained by systematic sales of Bitcoin holdings by miners (Section 3.2). This appendix presents complementary evidence on the feedback between mining investment, network security, and Bitcoin demand illustrated in Figure 1. We identify a separate Bitcoin demand shock jointly with the mining shock, investigate whether the endogenous hashrate response amplifies demand-shock propagation, and examine whether the response varies with prior mining stress. The joint identification also provides a useful check that the baseline mining shock is not materially contaminated by the demand disturbance captured by our second instrument.

Figure B.3: Robustness: IRFs to mining shock in daily VAR

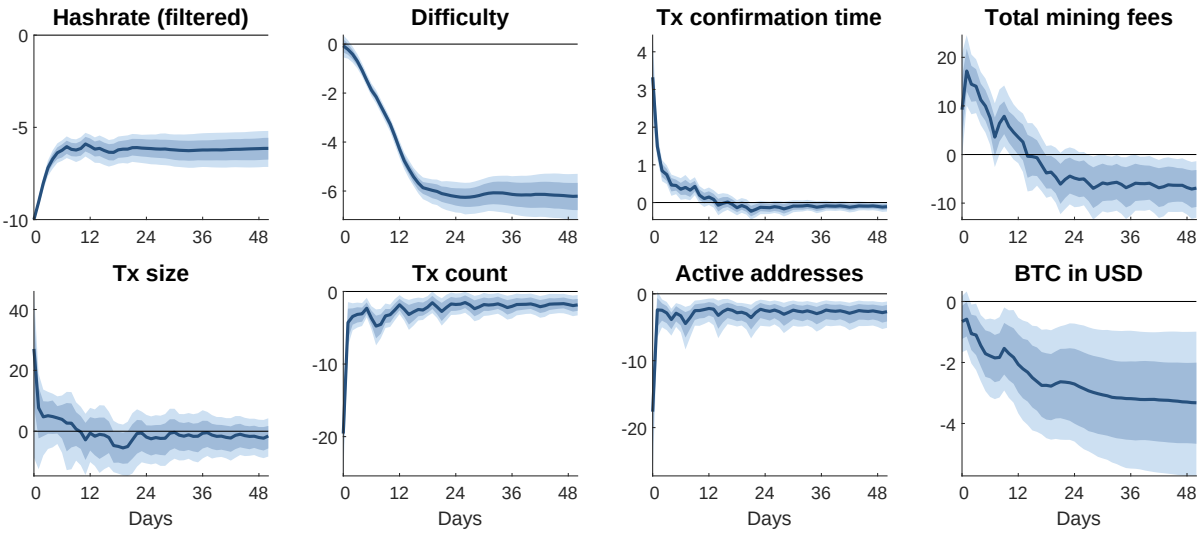

Note. Impulse responses to a mining shock in daily VAR, normalized to decrease the hashrate by 10 percent. Shaded areas denote 68% and 90% confidence bands. All values in percent, except for transaction confirmation time measured in minutes. Time sample: July 2013 to April 2026.

Adding a Bitcoin demand shock. A central feature of Bitcoin's economic design is that mining activity responds endogenously to the market value of Bitcoin. As the reward for adding new blocks is denominated in bitcoins, an increase in its price raises the profitability of mining and encourages miners to devote additional computational resources to the network. This is the "hashrate follows price" mechanism represented by the red arrow in Figure 1, which constitutes one side of the feedback relationship between prices and network security. We begin by providing direct empirical evidence for this relationship.

To do so, we identify a broad Bitcoin demand shock alongside our mining shock in the same proxy VAR. Specifically, we introduce a second external instrument intended to capture unexpected changes in Bitcoin demand or sentiment, in addition to the mining-disruption instrument employed so far. We construct the second instrument from the time-stamped events listed in Appendix Table A.2, selected for their potential effect on Bitcoin demand or market sentiment.[19]

Importantly, the two shocks are identified jointly rather than sequentially. With two external instruments, the proxy VAR identifies a two-dimensional structural impact space. Within this space, we select an optimal orthogonal rotation that makes the correlation matrix between instruments and structural shocks as diagonal as possible, minimizing the off-diagonal correlations relative to the diagonal ones.[20] The resulting shocks are thus

[19]For each event, we use minute-frequency BTC/USD prices to calculate the percentage price change from 60 minutes before to 60 minutes after its recorded time. We sum the event-window changes within each Monday-start week and set the instrument to zero in other weeks.

[20]The procedure follows the joint multi-instrument identification approach Karau (2026), which itself is an extension of the method developed in Piffer and Podstawski (2018).

distinguished by their respective associations with the mining and demand instruments, while allowing both to affect all variables in the system.

FIGURE B.4 compares impulse responses to the two identified shocks. Both are contractionary, with the mining shock normalized to reduce hashrate by 10 percent on impact and the Bitcoin demand shock normalized to lower Bitcoin prices by 10 percent. The responses reveal strikingly different dynamics. Following the demand shock, Bitcoin prices fall immediately and persistently, whereas hashrate initially responds very little. Instead, the decline in mining activity builds up gradually over subsequent months. This delayed adjustment is consistent with the presence of fixed costs and other frictions in mining investment and operation: lower Bitcoin valuations reduce mining profitability, but miners do not immediately adjust their computational resources. Hence, the results provide direct evidence for the endogenous response of mining activity to Bitcoin prices anticipated in Figure 1.

By contrast, an exogenous mining shock immediately lowers hashrate, while its effect on Bitcoin prices is initially small and builds up gradually. The shocks also differ in their effects on mining fees and transaction activity. In particular, the temporary disruption of block confirmation times and the associated adjustment of mining difficulty are characteristic of the mining shock, whereas the demand shock primarily affects transaction demand and mining profitability. These differences corroborate the distinction between exogenous changes in mining effort and endogenous mining adjustments following shifts in Bitcoin demand.

The joint identification also provides a useful robustness check of our baseline results. In principle, if our mining instrument systematically captured general Bitcoin demand disturbances, part of the previously identified mining shock could reflect such disturbances rather than exogenous changes in mining activity. Allowing the demand instrument to identify a separate structural direction could then materially alter the mining shock's estimated effects. FIGURE B.4, however, shows that the mining impulse responses remain remarkably similar to those obtained in the baseline single-instrument specification in FIGURE 4. This stability is not imposed by the identification procedure, since the optimal rotation is allowed to change the mining shock's impact vector. It therefore suggests that the original mining shock contains little of the demand component separately identified by the second instrument, lending further support to our interpretation of the baseline results.

FEEDBACK EFFECTS FROM MINING. Having established that Bitcoin demand shocks induce an endogenous, albeit delayed, adjustment of mining activity, we next investigate whether this response in turn affects Bitcoin valuations. This is a central implication of the feedback mechanism illustrated in Figure 1 and formalized in models such as Pagnotta (2022): changes in Bitcoin prices affect mining incentives, which alter the network's

Figure B.4: Mining and Bitcoin Demand Shocks

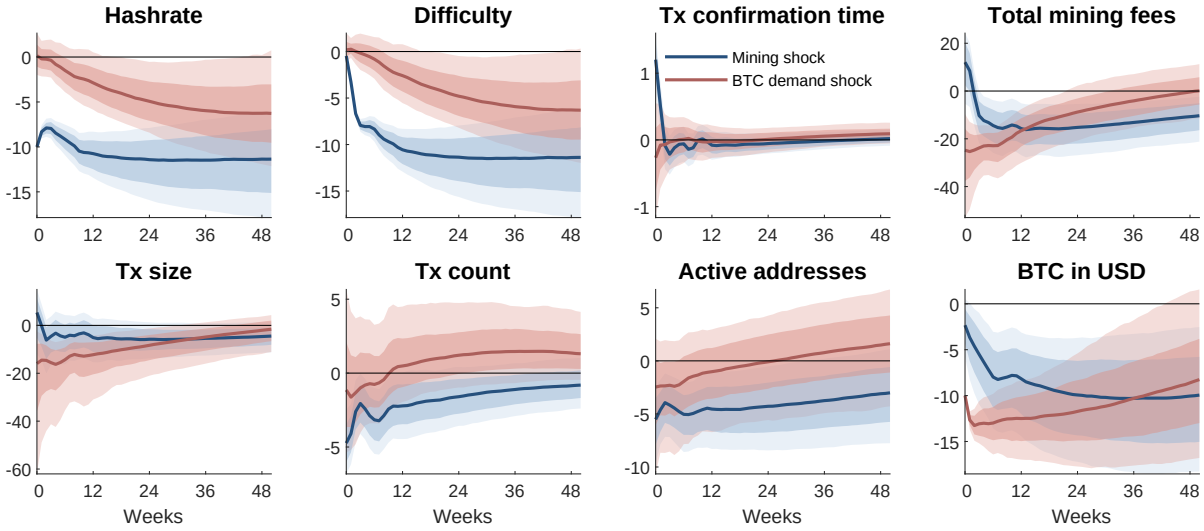

Note. Impulse responses to mining and Bitcoin demand shocks identified jointly in the same two-instrument proxy VAR, normalized to decrease the hashrate and the price of Bitcoin by 10 percent, respectively. Shaded areas denote 68% and 90% confidence bands. All values in percent, except for transaction confirmation time measured in minutes. Time sample: July 2013 to April 2026.

security and thereby feed back into user demand and prices. Consequently, the effect of a demand shock on Bitcoin valuations may be amplified by the endogenous response of mining activity.

We investigate this mechanism using a counterfactual exercise within the jointly identified two-shock VAR. Specifically, we consider the response to a negative Bitcoin demand shock under a hypothetical scenario in which the endogenous decline in hashrate is prevented. To construct this counterfactual, we introduce a sequence of offsetting mining shocks such that their combined contribution to hashrate exactly neutralizes the response induced by the initial demand shock at each horizon. All other variables are allowed to respond according to the estimated VAR dynamics. Comparing the resulting impulse responses with the unrestricted baseline therefore reveals how the endogenous adjustment of mining activity contributes to the propagation of the demand shock.

Figure B.5 presents the results. The solid lines show the baseline responses to the Bitcoin demand shock, while the dashed lines represent the counterfactual in which hashrate is held at its initial level. As intended, the counterfactual eliminates the endogenous decline in mining activity and the associated reduction in mining difficulty. More importantly, it substantially alters the response of Bitcoin prices. Whereas the baseline demand shock generates a persistent decline in valuations, prices recover considerably more quickly when the hashrate response is offset. The difference becomes increasingly pronounced over time, mirroring the gradual decline in mining activity documented above.

These findings indicate that the endogenous adjustment of mining activity is an important amplification mechanism for Bitcoin demand shocks. A decline in prices reduces

Figure B.5: Mining feedback and the propagation of demand Shocks

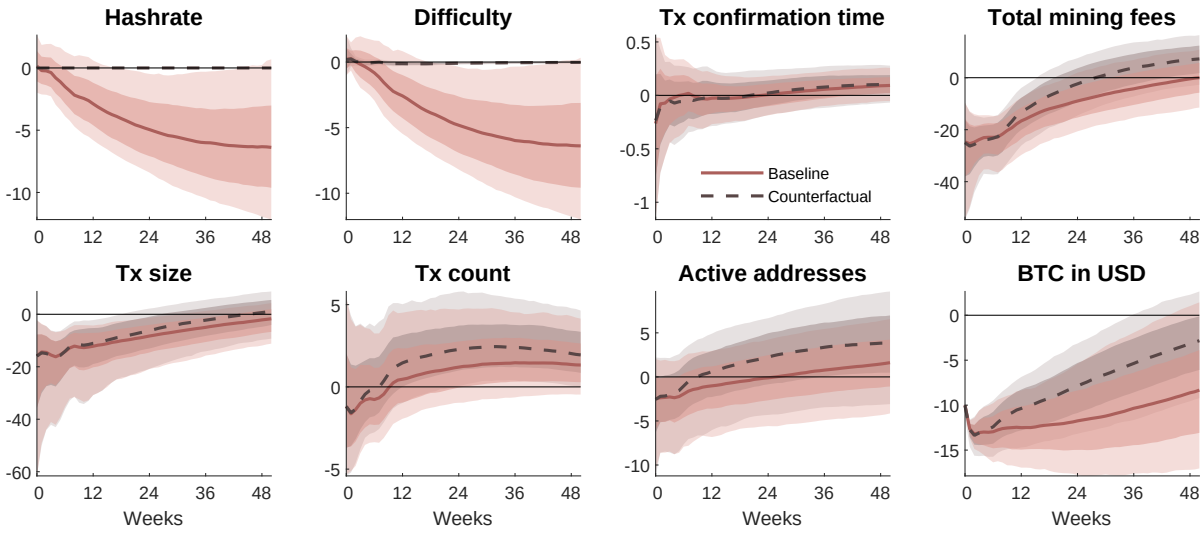

Note. Impulse responses to a negative Bitcoin demand shock identified jointly with the mining shock in the proxy VAR, normalized to decrease Bitcoin prices by 10 percent on impact. Solid lines show the baseline responses; dashed lines show a counterfactual in which the endogenous hashrate response is neutralized by a sequence of offsetting mining shocks. Shaded areas denote 68% and 90% confidence bands. All values in percent, except for transaction confirmation time measured in minutes. Time sample: July 2013 to April 2026.

mining incentives, and the resulting reduction in mining activity reinforces the initial deterioration in valuations. Conversely, preventing the decline in mining activity substantially attenuates the persistence of the price response. The counterfactual thus provides direct evidence for the economic importance of the feedback between mining and Bitcoin valuations. While the exercise does not separately identify changes in perceived network security, the results are consistent with the security mechanism through which mining activity sustains user demand and market valuations.

The role of mining stress. The security mechanism also implies that the strength of the feedback between mining and valuations may depend on the state of the mining network. In particular, a decline in Bitcoin demand may be more consequential when mining activity has already been adversely affected by previous disruptions. In such circumstances, further reductions in mining incentives may reinforce concerns about the sustainability of network security and hence have particularly pronounced effects on current valuations. Conversely, when mining activity is relatively resilient, a given decline in Bitcoin demand may have less persistent consequences.

We investigate this prediction using state-dependent local projections that allow the effects of Bitcoin demand shocks to vary with the degree of mining stress. Specifically, we interact the identified Bitcoin demand shock with a predetermined measure of mining stress derived from lagged mining shocks, and estimate the resulting response of Bitcoin prices over subsequent weeks. Using lagged identified mining disturbances to character-

Figure B.6: Bitcoin Demand Shocks and Mining Stress

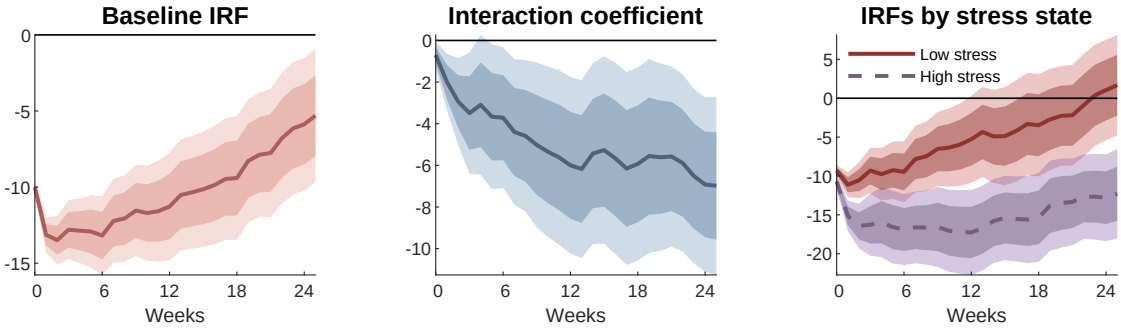

Note. Impulse responses of Bitcoin prices to a negative Bitcoin demand shock estimated using local projections, scaled such that it decreases the price of Bitcoin by 10% on impact. The left panel shows the unconditional response, the middle panel reports the interaction coefficient with lagged mining shocks, and the right panel shows the implied responses during periods of low and high mining stress. Shaded areas denote 68% and 90% confidence bands. Values in percent. Time sample: July 2013 to April 2026.

ize the state of the network is particularly useful because it reduces the concern that the measure of mining stress simply captures preceding changes in Bitcoin demand or valuations.[21]

Figure B.6 presents the results. The left panel shows the baseline local-projection response of Bitcoin prices to a negative demand shock, without conditioning on the state of mining activity. The middle panel reports the interaction coefficient with mining stress, which is consistently negative and indicates that adverse mining conditions amplify the negative valuation effects of demand shocks. The right panel illustrates the economic magnitude of this interaction by distinguishing between periods of low and high mining stress.

The difference is substantial. During periods of low mining stress, Bitcoin prices recover relatively quickly from an adverse demand shock. In contrast, when mining stress is elevated, the initial decline in valuations is followed by a much more persistent negative response. These findings suggest that the same deterioration in Bitcoin demand has considerably stronger consequences when the network has already experienced adverse mining disturbances.

This result complements the counterfactual exercise in Figure B.5. Whereas the counterfactual establishes that endogenous adjustments in mining activity amplify the propagation of demand shocks, the state-dependent estimates show that their effects are particularly pronounced when mining conditions are already unfavorable. Both findings are consistent with the security mechanism emphasized by Pagnotta (2022), in which user

[21] We construct mining stress from the identified mining shocks in the six weeks preceding each observation. We orient the shocks so that a positive innovation lowers hashrate on impact, sum the signed shocks from weeks $t-6$ through $t-1$, and standardize this sum. The low- and high-stress responses evaluate the estimated interaction at -1 and $+1$ of this standardized measure, respectively, rather than estimating separate subsamples.

Figure B.7: Mining and Demand Contributions to Bitcoin during 2020–21

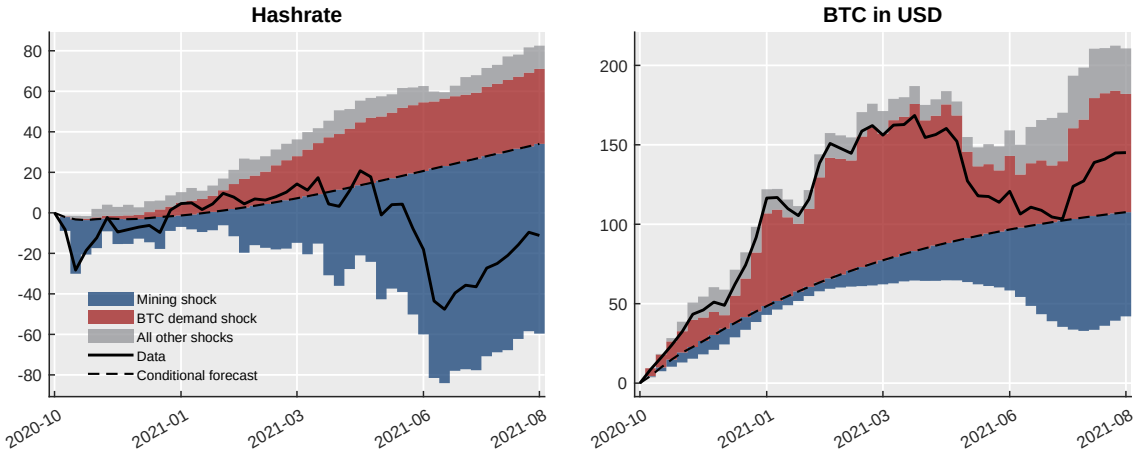

Note. Historical forecast error decomposition for 2020–21 from the jointly identified mining and Bitcoin demand shocks. The contributions are model-based and need not exhaust movements in Bitcoin prices; other structural disturbances and initial conditions can also matter.

demand, mining investment, and network security reinforce each other. Importantly, this mechanism need not require a substantial increase in the immediate probability of a successful attack. Even concerns about the future sustainability of mining activity and network security may be sufficient to affect current Bitcoin valuations. This provides additional support for the feedback mechanism underlying the dynamic model in Section 4.

The Chinese mining ban and the Bitcoin boom of 2020–21. The joint identification also helps interpret historical episodes in which mining and demand forces operated at the same time. A particularly instructive case is the Chinese mining crackdown of mid-2021. Mining operations had been heavily concentrated in China; widely cited estimates place the country's share of Bitcoin mining above 50% in early 2021 (Cambridge Centre for Alternative Finance, 2021). Restrictions and closures raised uncertainty about whether displaced operations could relocate promptly and recover their previous profitability, especially given differences in electricity costs and infrastructure across jurisdictions. In isolation, such an episode would tend to depress hashrate and could raise concerns about the longer-run viability of the mining network.

At the same time, Bitcoin experienced strong demand and substantial price increases during the broader 2020–21 period, against the backdrop of pandemic-era investment and cryptocurrency adoption (Auer et al., 2023). Stronger valuations can sustain mining incentives even while operations are being disrupted or relocated. Figure B.7 uses the jointly identified two-shock VAR to illustrate how mining-related and demand-related innovations exerted offsetting influences on Bitcoin prices around 2020-21. Whereas speculative demand pushed up prices during the early stages of the COVID pandemic, the disruptions related to the Chinese mining ban in mid-2021 are identified by the model as

contractionary mining shocks pushing hashrate down. This also put pressure on Bitcoin valuations, which were however stabilized by recurring strong demand. This supported mining profitability even under otherwise less favorable conditions as mining activity shifted to countries such as Kazakhstan, Russia, Iran and the United States. Through the lens of the theoretical model, this is consistent with dissipating investor concerns over mining viability which otherwise would have depressed prices.

C Theoretical Model

Our empirical results suggest that Bitcoin trading outcomes depend not only on the current level of mining activity via a *transaction-speed channel* but also on its expected persistence. An exogenous decline in hashrate temporarily slows block production, yet confirmation times normalize as mining difficulty adjusts. Bitcoin prices, by contrast, respond only modestly on impact and decline more substantially in subsequent weeks. Complementary evidence on Bitcoin demand shocks and endogenous mining–price feedback is presented in Appendix B.2. We now develop a stylized model that connects these observations to the security mechanism underlying Bitcoin's proof-of-work protocol, interpreting the persistent price responses to mining shocks as evidence of a *security channel*.

Our starting point is the complementarity between mining incentives, network security, and Bitcoin valuations emphasized by Pagnotta (2022). We first explain this mechanism in a static setting, including why it can sustain a high-security equilibrium but also make that equilibrium vulnerable. We then adapt the model in a dynamic setting and introduce persistent disturbances to mining capacity, incomplete information, and Bayesian learning about the ability of mining activity to recover. Importantly, the central mechanism in the dynamic model is not a large change in the immediate probability of a successful attack. Instead, investors revise the probability that a sufficiently secure mining network can be sustained in the future. The exercise is intended to rationalize the empirical response patterns, rather than to estimate a fully structural model or quantitatively reproduce the VAR impulse responses. The transition rules and learning equations are developed below, followed by calibration, numerical implementation, and the model experiment.

C.1 Reference Model: Bitcoin Asset Pricing With Mining

Here we describe an asset pricing model that features interactions among Bitcoin users, miners and a potential saboteur who may attempt to compromise the blockchain that give rise to multiple static equilibria. For additional details the reader is referred to Pagnotta (2022).

The model includes a continuum of n homogeneous investors who can produce and consume a perishable good, with the price of this good serving as the numeraire. These agents have the option to purchase Bitcoins at a price p_t, which they value due to the potential for uniquely beneficial exchange opportunities in a subsequent interim subperiod t'. The utility derived from holding Bitcoins is represented by a continuous, strictly increasing, and concave function $V(\cdot)$, which captures the value agents place on the opportunities provided by Bitcoin transactions.

There is a malicious agent, termed a saboteur, who poses a risk of a systemwide attack between periods t and t'. The outcome of such an attack is binary: either the network survives and a new block is added to the ledger, or the attack is successful, rendering Bitcoins entirely worthless. The probability of the network surviving an attack is denoted by $S \in (0,1)$, which is referred to as the security function, specified below.

In case the attack fails, in period $t+1$ investors can sell their Bitcoin holdings in a liquidation market at the uncertain price p_{t+1}. Following the notation in Pagnotta (2022) and defining E_t^1 as the expectations operator conditional on an unsuccessful attack, investors' expectation of future prices is $E_t p_{t+1} = S_t E_t^1 p_{t+1} + (1 - S_t) \times 0$. Denoting returns $R_{t+1} = E_t^1 \frac{p_{t+1}}{p_t}$ (with $R_{t+1} < \frac{1}{\delta S_t}$),[22] and time preference rate $\delta \in (0,1)$, investors maximize $c_{it} - l_{it} + E_t(V(B_{it}p_t) + \delta c_{i,t+1})$ subject to the budget constraints $B_{it}p_t + c_{it} \leq l_{it}$ and $c_{t+1} \leq B_{it}p_{t+1}$, where B_{it} is the non-negative amount of Bitcoins held and l_{it} are labor hours. Denoting $b_{it} = p_t B_{it}$ as real Bitcoin holdings, we can simplify the problem to:

$$\max_{b_{it} \geq 0} S_t(fV(b_{it}) + (1-f)\delta b_{it} R_{t+1}) - b_{it}, \tag{C.1}$$

where f is the probability with which holders find an exchange opportunity.

At the start of period t, miners invest in computational power to verify blocks and earn rewards. The share of blocks verified by a miner is proportional to their computational power contribution. The cost function for mining, $C(h)$, is assumed to be increasing and convex. Miners are risk-neutral, act as price takers, and form expectations about future Bitcoin prices. Hence, each miner j maximizes $P(h_j, h_{-j}) \cdot \delta\psi E_t^1[p_{t+1}] - C(h_j)$, where $-j$ denotes the other miners, δ is the time preference and ψ represents the block reward in bitcoins. Miners' optimal investment is then characterized by a symmetric Nash equilibrium, where the system's hashrate $H = hm$ is determined by individual investments in hashing h times the number of miners m:

$$H_t = \left(\frac{m(m-1)}{m^2}\right) \frac{\delta\psi}{\kappa} E_t^1[p_{t+1}] \tag{C.2}$$

in which for simplicity we have specified a linear cost function, i.e. $C'(h) = \kappa$. Equation (C.2) resembles a free-entry condition under which miners enter the market until rewards from mining break even with mining costs. Equation (C.2) therefore formalizes the red arrow in the introduction of the main text in FIGURE 1: an increase in mining revenues from a higher Bitcoin price leads to a rise in mining investment in equilibrium.

The presence of a saboteur introduces an aggregate source of risk, as a successful attack would affect all participants in the Bitcoin network. In the model, the saboteur is a single entity with a fixed budget that allows for a constant hashrate A. The likelihood of a successful attack by the saboteur in the interim period t' is modeled as a binomial

[22] If R_{t+1} were larger than $\frac{1}{\delta S_t}$, demand for Bitcoin would not be bounded.

random walk, with the probability of ultimately eliminating a deficit of k blocks given by $\left(\frac{A}{H_t}\right)^k$, provided the saboteur's hashrate is less than half of the total hashrate, and one otherwise.

The security function consistent with such a game between honest miners and the saboteur is then given by:

$$S(H_t, A) = \begin{cases} 1 - \left(\frac{A}{H_t}\right)^k & \text{if } H_t > A, \\ 0 & \text{else.} \end{cases} \tag{C.3}$$

This function captures the notion that the security of Bitcoin decreases as the hashrate controlled by the saboteur, A, approaches the total hashrate, H_t. The parameter k represents the minimum block length for a disruptive fork to lead to a collapse in Bitcoin demand.

The equilibrium price and security of Bitcoin are then jointly determined by the interaction of user demand, miner investment, and the saboteur's actions. Given market clearing, $nB_{it} = B$, optimal investor demand (C.1), the free-entry condition (C.2), and the security function (C.3), we can summarize the equilibrium conditions as:

$$S(H(p_t), A)\left(fV'\left(\frac{B}{n}p_t\right) + (1-f)\delta R_{t+1}\right) = 1 \tag{C.4}$$

An equilibrium requires that investors' marginal utility of Bitcoin trading opportunities and the discounted expected return R, adjusted for the level of network security, equals one. As the security level itself depends on the Bitcoin price, there is no unique equilibrium: a high perceived value of Bitcoin incentivizes miners to invest in computational resources, thereby increasing network security and supporting a high equilibrium price to begin with. Conversely, a low-security, low-price equilibrium is equally self-fulfilling.

We visualize equilibrium multiplicity in FIGURE 11. The red line depicts the security level S_t, governed by equation (C.3). Provided $H_t > A$, S_t increases in p_t since a higher Bitcoin price incentivizes miners to invest more resources into hashing. The blue line depicts the left-hand side of equation (C.4), labeled as $\Delta(p)$. If there were no security risks ($S_t = 1$), $\Delta(p)$ would fall monotonically in the current price of Bitcoin as capital returns decline. Yet, with sufficiently low levels of security for low Bitcoin prices, $\Delta(p)$ initially increases with Bitcoin valuations, and, as a result, security increases as well. Two equilibria can be found where the blue line equals unity: in one, both security and the current price are low (p_t^L, S_t^L), in the other both are high (p_t^H, S_t^H). Importantly, below a threshold price p_t^M, miners abstain from investing in mining such that $S_t = 0$ regardless of the current price. Also, if $A > H_t$, no positive-price equilibrium can exist: as sabotage would always be successful, there is no demand for Bitcoin and prices are zero. We will return to this point below.

C.2 Dynamic Extension: Mining Capacity, Persistence, and Bayesian Learning

We now extend the static framework of Section C.1 to allow for persistent mining disruptions and learning about their longer-run implications. Before introducing the dynamics, it is useful to show how the equilibrium conditions derived above lead to the tractable functional forms used in our quantitative model. In particular, these functional forms preserve the price–security–mining complementarity of Pagnotta (2022); the additional assumptions concern the adjustment of mining capacity, investors' information, and the future viability of the high-security equilibrium.

Consider first investors' demand for Bitcoin. As a special case of the preferences in Section C.1, let the utility from real Bitcoin holdings b be logarithmic, $V(b) = \nu \log b$, where $\nu > 0$. Substituting $V'(b) = \nu/b$ and the conditional expected return $R_{t+1} = E_t^1[p_{t+1}]/p_t$ into the investor equilibrium condition (C.4) yields

$$p_t = S(H_t)\Big[M + \chi E_t^1 p_{t+1}\Big], \qquad M \equiv \frac{f\nu n}{B}, \qquad \chi \equiv (1-f)\delta. \tag{D1}$$

where M captures the transaction-service value of Bitcoin and χ discounts its continuation value. Thus, our valuation equation follows directly from Pagnotta's investor problem under logarithmic utility; we subsequently extend the continuation value to allow for changes in the viability of the network. For a stationary high-security outcome, $E_t^1[p_{t+1}] = p_t = p$, and hence

$$\begin{aligned} S(H) &= \max\left\{0, 1 - \left(\frac{A}{H}\right)^k\right\}, \\ p^{\text{stat}}(H) &= \frac{S(H)M}{1 - \chi S(H)}. \end{aligned} \tag{M1}$$

The first line restates the security function from Section C.1: A denotes the saboteur's fixed computing power, k determines the attack-depth sensitivity, and H is the honest network hashrate. The second line gives Bitcoin's stationary price for a specified hashrate. In particular, the same security function enters both the static equilibrium geometry and the dynamic valuation problem below.

The mining side can be linked to the original framework equally directly. With linear marginal mining costs, the symmetric mining equilibrium (C.2) takes the form $H_t = \alpha E_t^1[p_{t+1}]$, where $\alpha \equiv [(m-1)/m]\delta\psi/\kappa$ summarizes mining rewards relative to costs. In a stationary equilibrium, normalize utilization so that hashrate equals installed mining capital, $H = K$. Then $K = \alpha p^{\text{stat}}(K)$. Writing $\alpha = r/c$, with $c > 0$ a normalization, this condition is equivalently

$$r(K) = c\,\frac{K}{p^{\text{stat}}(K)}, \qquad r(1) = 1. \tag{M2}$$

The function $r(K)$ gives the effective reward-to-cost ratio needed to sustain a particular amount of mining capital. The constant c fixes the reference normalization $r(1) = 1$. Because greater capital raises network security and hence Bitcoin's price, this required ratio is non-monotonic. It attains a minimum $r^* \equiv \min_{K>A} r(K)$: for a given ratio $r > r^*$, the stationary system has a lower and an upper capital root, denoted $K^L(r)$ and $K^H(r)$, whereas below r^* no positive high-capital solution exists. Both roots solve $r(K) = r$, but only the upper root is used as the desired high-security capital level. This reproduces the multiple-equilibrium structure illustrated in Figure 11. The lower root will serve as a viability boundary in the dynamic model; it is distinct from the absorbing low-value state introduced below.

We next allow mining conditions and rewards to evolve over time. As in the VAR, time is measured in weeks, and installed mining capital K_t is distinguished from the fraction a_t of that capital currently available for operation. As outlined below, a_t can be affected by mining disruptions. The stationary condition above determines a *target* for mining capital, rather than requiring capacity to adjust instantaneously.

To introduce dynamics, we distinguish between two dimensions of mining conditions. The first concerns the underlying resilience of the mining industry, represented by an unobserved state $\theta_t \in \{G, B\}$. In the resilient state G, mining activity can recover relatively quickly from disruptions and operating conditions remain favorable. In the fragile state B, recovery is slower and mining is less profitable. Investors cannot directly observe this state and must instead learn about it from the evolution of mining activity.

The second dimension concerns the economic environment in which mining takes place. We distinguish between the current reward regime ($e_t = 0$) and a potentially less favorable future regime ($e_t = 1$), characterized by lower effective mining rewards relative to costs. While both resilient and fragile mining conditions can sustain the high-security equilibrium under current rewards, the distinction becomes consequential when mining incentives weaken: resilient mining fundamentals may still support sufficiently high mining activity, whereas fragile conditions may no longer do so. The future transition to the stressed regime is uncertain, and we introduce its arrival probabilistically below.

The interaction between these two dimensions is central to our mechanism. Investors learn about the persistence of mining weakness following an initial disruption, and thereby revise the probability that Bitcoin can sustain its high-security equilibrium under less favorable future conditions. Such revisions affect current valuations even when mining activity remains sufficient to maintain a high degree of contemporaneous network security.

For either underlying state θ and reward regime e_t, let r_{θ,e_t} denote the corresponding baseline reward-to-cost ratio. We allow this ratio to vary with Bitcoin's price p_t, with elasticity $\eta_p > 0$. The resulting effective ratio determines a state-contingent desired

capital stock $K^T_{\theta,t}$, while installed capital K_t approaches that target only gradually:

$$\begin{aligned} \widetilde{r}_{\theta,e_t}(p_t) &= r_{\theta,e_t} \max\{p_t, \underline{p}\}^{\eta_p}, \\ K^T_{\theta,t} &= \begin{cases} K^H(\widetilde{r}_{\theta,e_t}(p_t))\,, & \text{if the high root exists,} \\ 0, & \text{otherwise,} \end{cases} \\ K^\theta_{t+1} &= K_t + \lambda^\theta_t\Big(K^T_{\theta,t} - K_t\Big). \end{aligned} \tag{M3}$$

Here $\underline{p} > 0$ is a small price floor in the profitability calculation, included to prevent numerical problems when the price approaches zero. The upper static capital root K^H comes from equation (M2); λ^θ_t is the speed at which current capital adjusts toward that target and may differ between investment and contraction. When the high root does not exist, the unconstrained capital target is zero. The dependence of the target on current price and the gradual-adjustment rule are reduced-form extensions of the original static mining equilibrium, rather than solutions to a separate intertemporal investment problem for miners. They allow adverse mining conditions and lower Bitcoin prices to impair the rebuilding of capacity over time, just as we observe in the data.

Finally, operational availability and utilization determine how installed capital translates into observed hashrate, while difficulty D_t responds with a delay. Importantly, investors cannot directly observe which mining state prevails and must infer it from the subsequent recovery of the network. We now specify these recovery dynamics and the associated Bayesian learning process.

Mining activity and recovery. The state governing investors' valuation at the beginning of week t is $X_t = (\pi_t, K_t, D_t, a_t, e_t)$, where $\pi_t = \Pr(\theta_t = G \mid \mathcal{I}_t)$ denotes the probability assigned to resilient mining fundamentals given information $\mathcal{I}_t$. The latent state follows a two-state Markov chain, with transition probabilities

$$\Pr(\theta_{t+1} = G \mid \theta_t = G) = p_{GG}, \qquad \Pr(\theta_{t+1} = G \mid \theta_t = B) = p_{BG}. \tag{M4}$$

Here p_{GG} is the probability that the resilient state persists into the next week, while p_{BG} is the probability of recovering from the fragile state to the resilient state. The associated stationary probability of the resilient state is $\bar{\pi} = p_{BG}/(1 - p_{GG} + p_{BG})$. The two states therefore differ not just in the speed with which a particular outage can be repaired, but also in the underlying economics of sustaining mining capacity. The state θ_t is not directly observed by investors. The transition probabilities and their implied persistence are discussed in the calibration subsection.

Given installed capital and operational availability, aggregate hashrate also depends on the share of available computing power that miners choose to utilize. We allow utilization to respond to the profitability of mining, which depends, among other things, on

the relationship between mining difficulty and the Bitcoin price. A higher difficulty level increases the expected computational effort required to obtain a block reward, whereas a higher Bitcoin price increases the value of that reward. Holding other factors constant, a rise in difficulty relative to the Bitcoin price therefore makes mining less attractive and may induce miners to temporarily deactivate equipment.

We capture this relationship through a simple reduced-form utilization rule. Specifically, we define

$$x_t = \max\left\{\frac{D_t}{\max\{p_t, \underline{p}\}} - 1, 0\right\}, \qquad u_{\theta,t} = \min\{1, \max\{\underline{u}, \bar{u}_\theta \exp(-\eta x_t)\}\}. \tag{M5}$$

The variable x_t measures the extent to which mining difficulty exceeds its reference level relative to the Bitcoin price, with both variables expressed in normalized units. When this ratio does not exceed one, $x_t = 0$ and utilization equals its state-dependent reference level $\bar{u}_\theta$. Otherwise, utilization declines exponentially with x_t, at a rate governed by $\eta > 0$. The minimum and maximum operators ensure that utilization remains between the lower bound $\underline{u}$ and one. The parameter $\underline{p}$ imposes a numerical floor on the price entering the profitability measure.

The state-specific reference utilization rates $\bar{u}_G$ and $\bar{u}_B$ allow operationally available capital to be used less intensively under fragile than under resilient mining fundamentals even in the absence of additional profitability pressure. The parameter η governs how strongly utilization responds to difficulty relative to the price; the bounds $\underline{u}$ and $\underline{p}$ limit utilization and stabilize the profitability calculation, respectively. The benchmark choices and their economic interpretation are discussed separately in Section C.4.

Aggregate hashrate is specified as

$$H_t = \frac{a_t K_t}{\bar{u}} \left[\pi_t u_{G,t} + (1 - \pi_t) u_{B,t}\right], \qquad \bar{u} \equiv \bar{\pi}\bar{u}_G + (1 - \bar{\pi})\bar{u}_B. \tag{M6}$$

Here $a_t K_t$ is the amount of installed capital currently available to mine, $u_{G,t}$ and $u_{B,t}$ are the utilization rates defined in equation (M5), and π_t is investors' posterior probability of resilient fundamentals. The normalization $\bar{u}$, calculated at the stationary belief $\bar{\pi}$, ensures that the reference capital and utilization levels coincide with the static relationship $H = K$ when the utilization penalty is inactive. The utilization rule is a tractable aggregate specification: since the underlying mining state is unobserved, we approximate aggregate utilization by its posterior-weighted value, using investors' assessment of resilient and fragile mining conditions. This reduced-form aggregation allows perceived mining conditions to influence contemporaneous utilization, while the realized latent state governs subsequent capital and operational recovery.

As introduced in equation (M3), capital adjusts only gradually toward the high-root target associated with the state-specific effective reward-to-cost ratio. We use different

speeds for expansions and contractions, setting

$$\lambda_t^\theta = \begin{cases} \lambda_{\text{in}}, & K_{\theta,t}^T \geq K_t, \\ \lambda_{\text{out}}, & K_{\theta,t}^T < K_t. \end{cases} \tag{M7}$$

Thus, λ_{in} governs how quickly additional equipment is installed when the capital target exceeds current capacity, and λ_{out} governs the contraction of capacity when the target is lower. In the benchmark, capacity can contract more quickly than it can be accumulated. In the numerical implementation, capital and its target are constrained to a finite grid; these computational bounds are described in Section C.4. The price dependence of the target, introduced above through $\widetilde{r}_{\theta,e_t}(p_t)$, provides a feedback channel from Bitcoin valuations to future mining capital.

As mentioned above, a negative mining disruption can make existing equipment unavailable without immediately removing it from the installed capital stock. We capture the subsequent restoration of operational capacity by

$$1 - a_{t+1}^\theta = \rho_\theta(1 - a_t), \qquad 0 < \rho_G < \rho_B < 1. \tag{M8}$$

The parameter ρ_θ measures the persistence of the operational shortfall $1-a_t$, with a higher value implying slower recovery of disconnected or impaired capacity. Since $\rho_B > \rho_G$, restoration is slower under fragile mining fundamentals. These laws deliberately allow a persistent mining response even before accounting for any endogenous adjustment induced by Bitcoin prices. Price feedback can reinforce that persistence by reducing utilization and discouraging capital accumulation, but does not generate all of it.

Finally, mining difficulty is predetermined within the week and adjusts to the prevailing hashrate according to

$$D_{t+1} = (1 - \delta_D)D_t + \delta_D H_t, \qquad 0 < \delta_D < 1. \tag{M9}$$

Here δ_D determines how quickly difficulty adapts to the current hashrate. This partial-adjustment rule approximates Bitcoin's protocol-specified retargeting of mining difficulty. The corresponding expected block interval is represented by $\tau_t = 10D_t/H_t$ minutes. A mining disruption initially raises τ_t because difficulty cannot adjust immediately. Subsequently, difficulty falls toward the lower hashrate, so block intervals normalize even when installed or operational mining capacity remains depressed. This separation between transaction processing and mining resources reproduces a central feature of the empirical impulse responses.

Learning from mining recovery. The economic significance of persistent mining weakness depends on what it reveals about the unobserved state θ_t. Investors know the

transition probabilities in (M4) and the state-contingent recovery laws, but do not observe the latent state itself. Each week they receive an imperfect signal about the recovery of mining activity and update their assessment of the network's resilience. In particular, define the next-period state-contingent normalized recovery measure

$$\widehat{H}_{\theta,t+1} = \frac{a^{\theta}_{t+1} K^{\theta}_{t+1} u_{\theta,t}}{\bar{u}}, \qquad s_{t+1} = \lambda_H \log \widehat{H}_{\theta_{t+1},t+1} + \varepsilon_{t+1}, \quad \varepsilon_{t+1} \sim \mathcal{N}(0, \sigma_s^2). \tag{M10}$$

The recovery measure $\widehat{H}_{\theta,t+1}$ is formed from next week's state-contingent availability a^{θ}_{t+1} and capital K^{θ}_{t+1}, together with current utilization $u_{\theta,t}$. The parameter λ_H scales the signal's responsiveness to recovery, while σ_s is the standard deviation of its noise. The realized signal is generated from the branch associated with the latent state at $t+1$. It is deliberately noisy, and need not coincide with an exact observation of every component of measured aggregate hashrate. This is important because the recovery of equipment, utilization, and mining profitability need not be separately observable or readily attributable to a particular mining disruption.[23]

The Bayesian update has two steps. First, before observing the signal, investors predict the probability of resilient fundamentals using the Markov transition probabilities:

$$\widetilde{\pi}_t = p_{GG}\pi_t + p_{BG}(1 - \pi_t). \tag{M11}$$

Second, conditional on the beginning-of-week state and the state-contingent recovery policies, the signal is normally distributed with mean $\mu_{\theta,t} = \lambda_H \log \widehat{H}_{\theta,t+1}$ and variance σ_s^2. Bayes' rule therefore yields

$$\pi_{t+1} = \frac{\widetilde{\pi}_t \varphi(s_{t+1}; \mu_{G,t}, \sigma_s^2)}{\widetilde{\pi}_t \varphi(s_{t+1}; \mu_{G,t}, \sigma_s^2) + (1 - \widetilde{\pi}_t)\varphi(s_{t+1}; \mu_{B,t}, \sigma_s^2)}, \tag{M12}$$

where $\varphi(s; \mu, \sigma^2)$ denotes the normal density with mean μ and variance σ^2. When the realized signal indicates a faster recovery than would be expected under fragile fundamentals, π_{t+1} tends to increase; unexpectedly weak recovery instead shifts probability toward the fragile state. Because the two states have different persistence and capital-adjustment characteristics, these posterior revisions affect expected mining conditions over many future weeks.

This learning mechanism is central to the model's interpretation of the empirical evidence. Investors can recognize a negative mining innovation immediately without knowing whether it reflects a short-lived interruption or a more persistent deterioration of mining conditions. Consequently, a large contemporaneous hashrate response need not

[23] The model uses a deliberately reduced-form information structure. Although capital and availability enter the pricing state, it does not separately update beliefs using all information that might be conveyed by exact observation of their state-contingent changes. The one-dimensional recovery signal is assumed to summarize the information relevant for learning about θ_t.

trigger a large price response. Subsequent evidence of weak recovery gradually changes beliefs about the network's long-run mining capacity and thus about future security.[24]

C.3 Future Mining Viability and Recursive Valuation

The remaining question is why learning about mining fundamentals can move Bitcoin prices appreciably if the immediate security of the network remains very high. The answer is that the mining–security complementarity described in Section C.1 can become more consequential when mining rewards fall relative to costs. In that case, the high-security equilibrium need no longer be viable. Investors' beliefs about the persistence of mining weakness therefore matter for the probability of sustaining the high-security outcome in the future, even if a successful attack is very unlikely today.

We retain the security function (C.3), restated as part of equation (M1), and normalize the reference hashrate to one. The saboteur's computational capacity A is constant. The benchmark chooses A and the attack-depth parameter k such that current network security remains extremely high at the reference hashrate, so the direct effect of a modest decline in current hashrate on contemporaneous security is very small.

To capture the potential vulnerability of the high-security outcome, we suppose that the economy can enter a persistently less favorable mining-reward environment. The indicator $e_t = 0$ denotes the initial reward regime and $e_t = 1$ the stressed regime. While $e_t = 0$, a viability test arrives with constant weekly hazard $h \in (0, 1)$, after which the stressed regime applies permanently to surviving high-security histories. Thus h determines the expected waiting time before a deterioration in the effective security budget, but the arrival of a test is neither a realized attack nor a deterministic Bitcoin subsidy halving. The benchmark value of h is described in Section C.4.

The stationary relationships in (M1)–(M2) provide a tractable test of whether the network can remain on the high-security branch after mining economics deteriorate. For a latent state $\theta \in \{G, B\}$, define

$$I_{\theta,t} = \mathbf{1}\Big\{K^L(\widetilde{r}_{\theta,1}(p_t)) \text{ exists and } K^{\theta}_{t+1} > K^L(\widetilde{r}_{\theta,1}(p_t))\Big\}. \tag{M13}$$

In other words, the price-adjusted reward-to-cost ratio in the stressed regime must admit a positive high-capital solution, and the amount of capital carried into the next period must lie above the associated lower-root boundary. If the stressed effective ratio is below the minimum r^*, no positive high-capital solution exists and the indicator is zero. The viability condition continues to apply in subsequent weeks once $e_t = 1$.

The two underlying mining states can therefore differ sharply in their ability to sup-

[24] In the numerical model the posterior is bounded away from zero and one for computational purposes, and expectations over the Gaussian signal are evaluated using numerical quadrature. These devices do not alter the Bayesian updating rule in (M12).

port the high-security outcome in the stressed regime, even if both support it under current mining rewards. We choose the benchmark reward ratios so that resilient mining fundamentals are compatible with a high-security solution under stress, whereas fragile fundamentals are not at the reference price. Because the effective ratios $\widetilde{r}_{\theta,e_t}(p_t)$ from equation (M3) also depend on the current Bitcoin price, the location of the viability boundary is endogenous. Lower prices weaken mining incentives and can make the high-security branch more difficult to sustain.

A history that fails this condition enters a separate absorbing low-value state L, with a constant residual Bitcoin price p_L. The value p_L is a calibrated modeling closure rather than being obtained by solving investors' and miners' problems in a low-security equilibrium.[25] The economic object priced by investors is the risk of losing the sustainable high-security outcome, rather than the likelihood of an attack actually occurring soon.

Subjective state transitions. We now combine the latent-state dynamics, recovery signals, and viability test into a distribution of future states. Recall that the public state is $X_t = (\pi_t, K_t, D_t, a_t, e_t)$. For any current state X and conjectured price policy $p(X)$, the Markov prediction in equation (M11) gives the probabilities $w_G(X) = \widetilde{\pi}$ and $w_B(X) = 1 - \widetilde{\pi}$ of the two *next-period* mining states. The signal density conditional on next-period state θ is $\varphi_\theta(s \mid X) = \varphi(s; \mu_\theta(X), \sigma_s^2)$, with mean implied by equation (M10). Let $\mathcal{B}(X, s)$ denote the posterior in equation (M12).

If the next mining state is θ, investors' possible next public state after receiving signal s and entering reward regime e' is

$$F_{\theta,e'}(X, s) = (\mathcal{B}(X, s), K_+^\theta, D_+, a_+^\theta, e'),$$

where K_+^θ, D_+, and a_+^θ are determined by the physical transition equations above. Define $q^0(e) = (1 - e)(1 - h)$ as the probability of remaining in the current reward regime without a viability test, and $q^1(e) = e + (1 - e)h$ as the probability that the stressed-regime viability condition applies (either because a test arrives or because the economy is already stressed). For any set $\mathcal{A}$ of surviving high-security states, the transition kernel is

$$\begin{aligned} Q_p(\mathcal{A} \mid X) = \sum_{\theta \in \{G,B\}} w_\theta(X) \int \varphi_\theta(s \mid X) \Big[& q^0(e) \mathbf{1}\{F_{\theta,0}(X, s) \in \mathcal{A}\} \\ & + q^1(e) I_\theta(X; p) \mathbf{1}\{F_{\theta,1}(X, s) \in \mathcal{A}\} \Big] \, ds, \end{aligned} \tag{M14}$$

$$q_L(X; p) = q^1(e) \sum_{\theta \in \{G,B\}} w_\theta(X) \Big[1 - I_\theta(X; p) \Big].$$

The indicator $I_\theta(X; p)$ is the high-branch viability condition in equation (M13); $q_L(X; p) =$

[25] In particular, L is different from the lower static capital root $K^L(r)$, which serves only as the boundary separating the high-capital branch from its failure region.

$1 - Q_p(\mathcal{X} \mid X)$ is the complementary probability of entering the absorbing state L, where $\mathcal{X}$ denotes the high-security state space. Once in L, the economy remains there and the price is $p(L) = p_L$. The explicit kernel makes clear that a mining state is selected according to the Markov transition, while the observed recovery signal changes beliefs about it.

Recursive Bitcoin valuation. The equilibrium price policy satisfies

$$p(X) = S(H(X, p(X))) \left\{ M + \chi \left[\int p(X')\, Q_p(dX' \mid X) + q_L(X; p) p_L \right] \right\}. \tag{M15}$$

Equivalently, in the discrete numerical state space, writing $Q_{ij}(p)$ for the transition probability from high-path node i to surviving high-path node j,

$$p_i = S(H_i(p_i)) \left[M + \chi \left(\sum_j Q_{ij}(p) p_j + \Big(1 - \sum_j Q_{ij}(p) \Big) p_L \right) \right]. \tag{D2}$$

The current security factor multiplies both the flow service value and the discounted continuation value, as it does in the static pricing equation. The dynamic extension additionally incorporates the possibility that future mining economics no longer support the high-security branch. Conditional on a successful continuation of the high branch, investors expect the future price policy $p(X')$, and otherwise, they receive the residual low-state value.

The weekly service-flow parameter M and continuation coefficient χ are derived from the investors' preferences in equation (D1). Their benchmark values, including the conversion from annual to weekly frequency and the normalization of the reference price, are collected in Section C.4.

Equation (M15) is nonlinear. The price policy affects utilization, the target capital stock, the distributions of future recovery signals, and the viability condition. These effects, in turn, change the discounted value on the right-hand side of the pricing equation. We solve for a fixed point in the price policy using a grid over the posterior, capital, difficulty, availability, and reward regime.

To summarize, equations (M1)–(M15), together with the exogenous parameter values and the initial state, form a closed recursive model: they determine static viability roots, physical mining outcomes, belief updating, high-branch transition probabilities, and the Bitcoin price.

C.4 Calibration and Numerical Implementation

We calibrate the model at weekly frequency to illustrate a mechanism rather than estimate its structural parameters or reproduce the full quantitative magnitude of the VAR

Table C.1: Benchmark calibration of the dynamic mining-security model

Component	Parameter values	Interpretation
Valuation	$\beta_A = 0.95$, $f_A = 0.50$, $p_L = 0.25$	Annual discounting and transaction services; residual low-state value
Current security	$S_0 = 0.999995$, $k = 2$	Near-certain survival / very high current security
Mining fundamentals	$p_{GG} = 0.99925$, $p_{BG} = 0.010$	Persistent good/bad states
Utilization	$\bar{u}_G = 1$, $\bar{u}_B = 0.88$, $\eta = 0.12$	Lower reference use under fragility; moderate price/difficulty response
Utilization and price floors	$\underline{u} = 0.45$, $\underline{p} = 0.05$	Bounds for numerical stability and high-branch operation
Capital adjustment	$\lambda_{\text{in}} = 0.010$, $\lambda_{\text{out}} = 0.040$, $\eta_p = 0.15$	Slow entry, faster exit, price feedback
Availability	$\rho_G = 0.55$, $\rho_B = 0.95$	Rapid vs. slow recovery of disabled equipment
Difficulty	$\delta_D = 0.55$	Partial weekly approximation to difficulty retargeting; approximates Bitcoin's ∼2-week difficulty adjustment
Recovery information	$\lambda_H = 0.40$, $\sigma_s = 0.075$	Moderately informative, noisy public signal
Current reward ratios	$r_{G,0} = 1.04$, $r_{B,0} = 0.60$	Both exceed the static viability threshold
Stressed reward ratios	$r_{G,1} \simeq 0.04952$, $r_{B,1} \simeq 0.03602$	Resilient state above, fragile state below the reference threshold
Viability-test arrival	$h = 1/(52 \cdot 4)$	Mean waiting time of four years

impulse responses. We distinguish parameters tied to the static equilibrium structure and Bitcoin's protocol from those governing reduced-form adjustment, information, and equilibrium viability. Table C.1 collects the benchmark values.

Valuation and equilibrium geometry. Following the transactional-demand and security complementarity in Pagnotta (2022), we choose an annual discount factor of $\beta_A = 0.95$ and an illustrative annual probability $f_A = 0.50$ of a transaction-service

opportunity. Their weekly counterparts are

$$\beta = \beta_A^{1/52}, \qquad f = 1 - (1 - f_A)^{1/52}, \qquad \chi = (1 - f)\beta, \qquad M = \frac{1}{S_0} - \chi. \tag{C1}$$

The last condition fixes the service-flow scale so that $p^{\text{stat}}(1) = 1$ when $S(1) = S_0$. We set $S_0 = 0.999995$ and $k = 2$, hence $A = (1-S_0)^{1/k}$ for the security function in equation (M1). The very high reference security is a device for studying a valuation effect that operates mainly through future viability, not through a quantitatively large contemporary attack probability. The attacker parameter and curvature should not be interpreted as estimates of the probability of a successful real-world Bitcoin attack. With these normalizations, the static ratio function in equation (M2) reaches $r^* \simeq 0.0377594$ at $K^* \simeq 0.019151$.

Mining incentives and adjustment. The reference ratios $r_{G,0} = 1.04$ and $r_{B,0} = 0.60$ place both latent mining states comfortably above the static minimum in the current reward regime. The stressed ratios $r_{G,1} \simeq 0.0495222 = 1.3115r^*$ and $r_{B,1} \simeq 0.0360161 = 0.9538r^*$ deliberately place the two states on opposite sides of the high-equilibrium viability threshold at the reference price. These choices isolate the economic role of learning: weak recovery is informative about whether mining can remain viable when future rewards become less attractive. They are illustrative rather than estimates of how an actual subsidy reduction changes mining profitability. The elasticity $\eta_p = 0.15$ adds moderate feedback from prices to capital targets. Weekly entry and contraction speeds of 0.010 and 0.040, respectively, represent the difficulty of rapidly installing new specialized mining equipment and the greater ease of withdrawing existing capacity. The asymmetry is economically motivated by adjustment frictions.

For utilization, $\bar{u}_G = 1$ and $\bar{u}_B = 0.88$ imply a 12-percentage-point reference gap in the use of operationally available computing capacity. With $\eta = 0.12$, doubling the difficulty-to-price ratio relative to its normalized value reduces desired utilization by approximately 11%, absent binding bounds. The lower utilization bound $\underline{u} = 0.45$ prevents the high-security branch's utilization rule from collapsing to zero within the computed state region. The price floor $\underline{p} = 0.05$ is a numerical regularizer.

Persistence, learning, and protocol adjustment. The hidden-state transition probabilities $p_{GG} = 0.99925$ and $p_{BG} = 0.010$ imply a stationary resilient-state probability $\bar{\pi} \simeq 0.93023$ and a mean fragile spell of $1/p_{BG} = 100$ weeks. Together with the recovery coefficients $\rho_G = 0.55$ and $\rho_B = 0.95$, they represent a large difference between temporary physical outages and persistent mining weakness. For example, absent other changes, the unavailability gap falls by 45% per week in the resilient state but by only 5% in the fragile state. These values ensure that subsequent hashrate recovery can convey information about latent mining resilience; the speed of that recovery is partly calibrated rather than

fully generated by endogenous price feedback. We choose $\lambda_H = 0.40$ and $\sigma_s = 0.075$ to make the public recovery signal informative but noisy, allowing investors to revise beliefs over time instead of immediately learning the latent state.

Bitcoin's protocol periodically retargets difficulty toward a roughly ten-minute block interval (Nakamoto, 2008). Rather than model the exact discrete 2,016-block schedule, we approximate it at weekly frequency with $\delta_D = 0.55$. This coefficient is chosen to generate an adjustment over the first few weeks. The model's expected block interval at any state is $\tau_t = 10D_t/H_t$ minutes. For valuation risk, we assume a constant viability-test hazard of $h = 1/(52 \cdot 4)$, corresponding to a mean wait of four years; this is a hypothetical stress-arrival process rather than the deterministic timing of Bitcoin halvings. We set the absorbing low-state price to $p_L = 0.25$. motivated by substantial obseved price reductions of successfully attacked cryptocurrencies.

Numerical solution. We solve the nonlinear price fixed point in equation (M15) on a tensor grid for (π, K, D, a, e), with 10 nodes for beliefs, 14 for capital, 9 for difficulty, 5 for availability, and two reward regimes (12,600 states). The continuous components of future states are interpolated, and signal expectations are evaluated with three-node Gaussian quadrature. The posterior is clipped to $[0.001, 0.999]$ on this grid. For each candidate price vector, current hashrate and branch-specific transitions are recalculated, the transition matrix is assembled, and the resulting Bellman system is solved until the fixed point converges. We distinguish this subjective price policy from the simulation of actual shock histories, in which the hidden mining state follows its Markov law. The finite-grid bounds, interpolation, quadrature, and convergence criteria are numerical choices and do not provide additional economic equilibrium conditions.

C.5 Modelling a Mining Disruption

We now use the calibrated dynamic model to illustrate how an exogenous disruption to mining activity can produce a persistent decline in Bitcoin valuations even when its immediate effect on network security is small. The model itself is fully specified by equations (M1)–(M15), and its benchmark parameters are summarized in Section C.4. The exercise below specifies an initial mining event, the information investors receive about it, and the distribution of histories used to calculate model responses. These are assumptions about the experiment rather than additional equilibrium conditions.

The mining event and information at impact. Before the disruption, the public state is $X_0^{\text{base}} = (\bar{\pi}, 1, 1, 1, 0)$, where $\bar{\pi}$ is the stationary probability of resilient mining fundamentals, $K_0 = 1$ denotes normalized installed capital, $D_0 = 1$ is the initial difficulty level, $a_0 = 1$ indicates fully available equipment, and $e_0 = 0$ denotes the current mining-

reward regime. The actual hidden mining state $\theta_0 \in \{G, B\}$ is initially distributed according to the same stationary Markov probabilities. We consider an event that reduces the fraction of operationally available capital from $a_0 = 1$ to $a_0^{\text{shock}} = 0.90$ without immediately changing installed capital or mining difficulty. Because mining difficulty is predetermined on impact, the loss of available equipment translates into an immediate decline in hashrate and a temporary increase in expected block times.

The occurrence of this physical disruption is assumed to be independent of the underlying resilient or fragile state. The event is nevertheless accompanied by adverse public information m about mining conditions. Although the realization of the information is observed by investors, its informational content is limited: its likelihood is moderately higher when mining fundamentals are fragile. Specifically, we assume

$$\Pr(m \mid \theta_0 = G) = 0.50, \qquad \Pr(m \mid \theta_0 = B) = 0.75. \tag{E1}$$

Let $b_0 = 1 - \bar{\pi}$ denote investors' pre-event probability of fragile fundamentals. Upon receiving the information, they update this probability according to Bayes' rule,

$$\begin{aligned} b_m \equiv \Pr(\theta_0 = B \mid m) = \frac{b_0 \Pr(m \mid B)}{(1 - b_0)\Pr(m \mid G) + b_0 \Pr(m \mid B)} \simeq 0.1011, \\ \pi_0^{\text{shock}} = 1 - b_m \simeq 0.8989. \end{aligned} \tag{E2}$$

Thus, the disruption and its accompanying information m lower the public probability of resilient mining fundamentals only modestly: investors' perceived probability of fragility rises from approximately 7% to 10%. The initial price $p(X_0^{\text{shock}})$ is determined by the equilibrium policy in equation (M15), using this *public* posterior and the reduced availability $a_0^{\text{shock}} = 0.90$.

A modest initial belief revision does not by itself imply that subsequent recovery must be modestly impaired. To illustrate the possibility that an initially ambiguous disruption is followed by persistently weak recovery, we examine a selected class of event histories. Let $Z = 1$ indicate an unobserved severity characteristic of an event. Conditional on the adverse information m, this characteristic is more likely to accompany fragile than resilient fundamentals:

$$\Pr(Z = 1 \mid m, G) = 0.10, \qquad \Pr(Z = 1 \mid m, B) = 0.60. \tag{E3}$$

The analyst conditions the reported model responses on m and $Z = 1$. For such histories, Bayes' rule implies that the initial *actual* probability of fragile fundamentals is

$$b_{mZ} \equiv \Pr(B \mid m, Z = 1) = \frac{b_m \Pr(Z = 1 \mid m, B)}{(1 - b_m)\Pr(Z = 1 \mid m, G) + b_m \Pr(Z = 1 \mid m, B)} \simeq 0.4030. \tag{E4}$$

Accordingly, the selected histories have an initial actual probability of resilient fundamentals of $1 - b_{mZ} \simeq 0.597$, substantially below the investors' public posterior $\pi_0^{\text{shock}} \simeq 0.899$. This difference is central to the experiment: investors observe the availability loss and information m, but *not* the indicator Z. They therefore cannot immediately infer that the particular class of histories shown in the figure is disproportionately associated with fragile mining conditions. As they subsequently observe recovery signals, their beliefs can move substantially toward the underlying distribution of mining fundamentals in the selected histories.

The indicator Z is an *event-selection device*, not another state variable in the equilibrium price policy or an additional innovation entering the physical transition equations. In particular, selection on Z changes the initial mixture of actual resilient and fragile states but does not change their subsequent Markov transition probabilities, the state-dependent recovery laws, or the information available to investors. Both the likelihoods of information m and the selection probabilities are illustrative choices. We do not assume that our empirical narrative instrument identifies Z or that the model experiment represents the unconditional response to all observed mining disruptions.

Propagation of actual and perceived states. The equilibrium policy $p(X)$ is solved using the *subjective* transition kernel Q_p in equation (M14). To evaluate the experiment, we must also propagate the *actual* latent state alongside the public state $X_t = (\pi_t, K_t, D_t, a_t, e_t)$. The true mining state evolves according to the Markov probabilities in equation (M4). Let T_G and T_B denote the state-contingent transition operators on surviving high-security public states, including the recovery signal and physical transitions for the respective *next-period* latent state. With rows indexed by the current latent state (G, B) and columns by the next latent state (G, B), the joint transition operator is

$$\mathcal{T} = \begin{pmatrix} p_{GG}T_G & (1 - p_{GG})T_B \\ p_{BG}T_G & (1 - p_{BG})T_B \end{pmatrix}. \tag{E5}$$

This operator preserves serial dependence in the actual mining state while investors update their beliefs using the noisy recovery signal in equation (M12). Any probability mass failing the future viability condition in equation (M13) enters the absorbing low-value state L. The simulated paths therefore average over distributions of possible realizations, not over a single deterministic recovery trajectory.

For any level variable Y_t, we report the percentage response of its expected level

relative to the corresponding unshocked distribution,

$$\mathrm{IRF}_Y(t) = 100\left(\frac{\mathbb{E}^{\mathrm{shock}}[Y_t \mid N_t]}{\mathbb{E}^{\mathrm{base}}[Y_t \mid N_t]} - 1\right), \qquad N_t = \{\text{no viability test through week } t\}. \tag{E6}$$

The superscripts distinguish the selected shocked distribution, conditional on m and $Z = 1$, from the stationary unshocked benchmark. Changes in the posterior π_t are instead reported in percentage points. Importantly, these distributions differ in their initial latent-state composition as well as the publicly observed mining event. Hence the plotted responses illustrate the behavior of a selected class of mining disturbances, rather than identifying an unconditional average causal effect of the availability loss alone.

The benchmark figure reports these responses over the first 52 weeks *conditional on no future viability test actually occurring during that period.* To construct the paths, we propagate the no-test part of the actual transition operator, conditional on the event not arriving. This conditioning is imposed on the *realized histories only.* Investors' equilibrium price policy still incorporates the strictly positive test hazard h described in Section C.4; they continue to price the possibility that future mining rewards may become insufficient to sustain the high-security equilibrium. The conditioning therefore isolates valuation changes *before* a realized transition to the stressed regime.

For comparison, the unconditional expected price also includes histories in which the viability test has occurred and the high-security branch may already have failed. For either the shocked or baseline distribution, it can be written as

$$P_t^{\mathrm{full}} = v_t P_t^{\mathrm{high}} + (1 - v_t)p_L, \tag{E7}$$

where v_t is the probability of still being on the high-security branch at horizon t, P_t^{high} is the mean price conditional on remaining on that branch (including histories in the stressed regime that have survived), and p_L is the residual value after its failure. The unconditional price, the price conditional on surviving high-security histories, and the no-test price shown in the benchmark figure are distinct objects. Differences between them should not be interpreted as an additive decomposition of transmission channels.

Alternative conditioning and survival paths. Figure C.1 compares the benchmark no-test responses with alternative ways of averaging over future viability outcomes. In the first seven panels, the benchmark paths (conditional on no test being realized through the respective horizon) are contrasted with paths conditional on still being on the high-security branch under the full stochastic test process. The latter group can include histories in which the one-off test has already occurred and the network survived. These are therefore *survivor-conditioned* responses, not equilibrium responses obtained by setting the viability hazard to zero. The price panel also reports the full, unconditional

Figure C.1: Model Responses under Alternative Survival and Conditioning Conventions

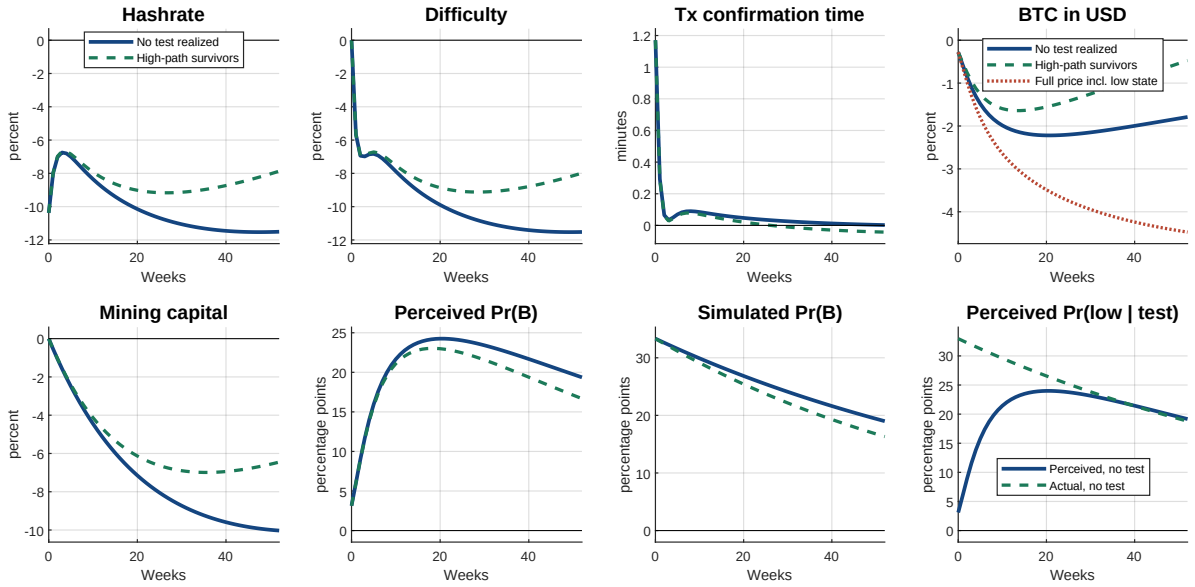

Note. Responses to the calibrated negative mining disruption relative to the unshocked benchmark. The first seven panels compare histories with no realized viability test to histories conditional on survival of the high-security branch under the full test process; the latter can include a test that has already been passed. The Bitcoin-price panel additionally reports the full unconditional average, assigning p_L to histories in the absorbing low-value state. Unconditional paths for mining variables are omitted because their outcomes after entry into that state are not modeled. Hashrate, difficulty, mining capital, and Bitcoin price are percentage deviations; confirmation time is the difference in expected minutes, and probability panels report percentage-point differences. The last panel instead contrasts investors' perceived and the simulated actual probabilities of entering the low-value state *conditional on a test*, both evaluated along no-test histories. These per-test risks are not unconditional weekly collapse probabilities. All price policies incorporate the positive prospective test hazard; the plotted price curves reflect distinct conditioning conventions rather than additive transmission channels.

expected price, which assigns the residual value p_L to histories already in the absorbing low-value state. In contrast, unconditional averages of hashrate, difficulty, block intervals, and other mining variables are not reported: the model specifies a price, but does not solve these physical outcomes, after entry into L.

The final panel compares investors' *perceived* and the simulated *actual* probabilities of failing the high-security viability condition *conditional on a test*, evaluated along the same no-test paths. The perceived measure is obtained from the subjective probability mass assigned to low-state transitions divided by the weekly test-arrival hazard; the actual measure uses the corresponding latent-state transition probabilities. These are conditional probabilities, not unconditional weekly collapse risks, and the gap between them reflects the selected event histories and investors' incomplete information. Since histories that have already survived a test are in a different reward regime, the corresponding conditional risk on the high-path-survivor population is not directly comparable and is not plotted. In particular, the three price responses represent different conditioning conventions, *not* additive components of a structural transmission decomposition.